

Rethinking Importance Weighting for Transfer Learning

Nan Lu^{*} Tianyi Zhang[†] Tongtong Fang[‡] Takeshi Teshima[§] Masashi Sugiyama[¶]

Abstract

A key assumption in supervised learning is that training and test data follow the *same* probability distribution. However, this fundamental assumption is not always satisfied in practice, e.g., due to changing environments, sample selection bias, privacy concerns, or high labeling costs. *Transfer learning* (TL) relaxes this assumption and allows us to learn under distribution shift. Classical TL methods typically rely on *importance-weighting*—a predictor is trained based on the training losses weighted according to the importance (i.e., the test-over-training density ratio). However, as real-world machine learning tasks are becoming increasingly complex, high-dimensional, and dynamical, novel approaches are explored to cope with such challenges recently. In this article, after introducing the foundation of TL based on importance-weighting, we review recent advances based on *joint* and *dynamic* importance-predictor estimation. Furthermore, we introduce a method of *causal mechanism transfer* that incorporates causal structure in TL. Finally, we discuss future perspectives of TL research.

1 Introduction

Supervised learning has been successfully applied to a wide variety of fields [1]. The vast majority of supervised learning methods follow the canonical framework of *empirical risk minimization* (ERM) [2, 3, 4, 5, 6, 7, 8], assuming that the samples used for training and the samples used for testing follow the *same* probability distribution. However, this assumption may not be fulfilled in many real-world scenarios. For example, due to changing environments, autonomous cars trained in good weather also need to work well in bad weather [9, 10]; due to sample selection bias, the training set may be gender or race imbalanced and the test set is balanced [11, 12]; and due to privacy concerns or high labeling costs, the labels of the training data may be corrupted or noisy versions of the ground truth [13, 14]. Such distribution mismatches may significantly degrade the prediction performance of models trained by standard supervised learning [15, 16].

^{*}The University of Tokyo, email: lu@ms.k.u-tokyo.ac.jp

[†]The University of Tokyo / RIKEN, email: zhang@ms.k.u-tokyo.ac.jp

[‡]The University of Tokyo, email: fang@ms.k.u-tokyo.ac.jp

[§]The University of Tokyo / RIKEN, email: teshima@ms.k.u-tokyo.ac.jp

[¶]RIKEN/ The University of Tokyo, email: sugi@k.u-tokyo.ac.jp

Fortunately, *transfer learning* provides us useful tools to learn under differing distributions. Classical transfer learning methods mainly rely on *importance weighting* [17, 18, 19], which handles the distribution mismatch in two steps [20, 12, 21, 22, 23, 24, 25, 26, 27]:

- *importance estimation*: estimate the ratio between test and training densities, a.k.a. the *importance*;
- *importance-weighted ERM*: train a predictive model by weighting the training losses according to the importance in the ERM framework.

These classical methods work well, as if there is no distribution mismatch, if the form of data is simple, e.g., some linear model suffices [28]. However, nowadays, as the data become increasingly complex, high-dimensional, and dynamical, new challenges arise in transfer learning.

1. First, given very complex and high-dimensional data, estimating the test-over-training density ratio becomes significantly difficult. However, for the classical two-step methods, the error occurred in the first importance estimation step directly propagates to the second importance-weighted training step, which degrades the performance of the learned predictor. Can we avoid this problem and use importance weighting to solve transfer learning problems in an end-to-end fashion?
2. Second, existing transfer learning researches mainly rely on certain assumptions on distribution shifts [16, 29]. However, the type of distribution shift can be unknown or multiple type of distribution shifts can present together. In practice, data from different domains may share a common data-generating mechanism, e.g., the source and target distributions are induced by a common causal mechanism. Can we leverage such causal mechanisms to tackle the transfer learning problem?

In this article, we answer these questions affirmatively and provide our solutions. In Section 2, we formulate the ordinary supervised learning and transfer learning problems. In Section 3 and Section 4, we review classical two-step importance weighting based methods for transfer learning. In Section 5, we answer the first question by proposing a one-step *joint* approach which integrates the importance estimation step and the importance-weighted ERM step by minimizing an upper bound of the test risk [30, 31]. In Section 6, we further explore the first question by proposing an end-to-end *dynamic* approach that iterates between importance estimation and importance-weighted ERM and combines them in a seamless manner. In Section 7, we answer the second question by proposing a causal mechanism transfer approach that incorporates the causal structure in transfer learning. We conclude this article and discuss future works in Section 8.

2 Problem Formulation

In this section, we introduce the problem setups for ordinary supervised learning and transfer learning.

2.1 Ordinary Supervised Learning

Let us consider the *supervised learning* problem of estimating an unknown input-output relationship from training samples. Let $\mathcal{X} \subset \mathbb{R}^{d_{\text{in}}}$ be the input feature space, and \mathcal{Y} be the output label space where $\mathcal{Y} \subset \mathbb{R}$ for regression, $\mathcal{Y} := \{+1, -1\}$ for binary classification, and $\mathcal{Y} := [k]$ for multi-class classification. Here, d_{in} denotes the input dimension, k (≥ 3) denotes the number of classes, and $[k] := \{1, 2, \dots, k\}$. Let $\mathcal{D}_{\text{tr}} := \{(\mathbf{x}_i^{\text{tr}}, y_i^{\text{tr}})\}_{i=1}^{n_{\text{tr}}}$ be the training samples in the source domain, where n_{tr} is the training sample size, $\mathbf{x}_i^{\text{tr}} \in \mathcal{X}$ and $y_i^{\text{tr}} \in \mathcal{Y}$ are the training input and output drawn independently from a source domain density $p_{\text{tr}}(\mathbf{x}, y)$. Any $p_{\text{tr}}(\mathbf{x}, y)$ can be decomposed in two ways, using either

- the class conditional density $p_{\text{tr}}(\mathbf{x} \mid y)$ and the class prior probability $p_{\text{tr}}(y)$, i.e., $p_{\text{tr}}(\mathbf{x}, y) = p_{\text{tr}}(\mathbf{x} \mid y)p_{\text{tr}}(y)$;
- the marginal density $p_{\text{tr}}(\mathbf{x})$ and the class posterior probability $p_{\text{tr}}(y \mid \mathbf{x})$, i.e., $p_{\text{tr}}(\mathbf{x}, y) = p_{\text{tr}}(\mathbf{x})p_{\text{tr}}(y \mid \mathbf{x})$.

Let $(\mathbf{x}^{\text{te}}, y^{\text{te}})$ be a test sample in the target domain, where $\mathbf{x}^{\text{te}} \in \mathcal{X}$ and $y^{\text{te}} \in \mathcal{Y}$ are the test input and output drawn from a target domain density $p_{\text{te}}(\mathbf{x}, y)$. Note that the test sample is not given in the training phase, but will be given in the test phase in the future.

The goal of supervised learning is to learn a predictor $f: \mathcal{X} \rightarrow \mathbb{R}^{d_{\text{out}}}$ that minimizes the expected test error, also known as the *risk*:

$$R(f) := \mathbb{E}_{(\mathbf{x}^{\text{te}}, y^{\text{te}}) \sim p_{\text{te}}(\mathbf{x}, y)} [\ell(f(\mathbf{x}^{\text{te}}), y^{\text{te}})]. \quad (1)$$

Here, $d_{\text{out}} = 1$ for regression and binary classification, and $d_{\text{out}} = k$ for multi-class classification. \mathbb{E} denotes the expectation, and ℓ denotes a real-valued *loss function* that measures the discrepancy between the true output value y and its predicted value $f(\mathbf{x})$. Typically, the predicted output is given by

$$\hat{y} = \begin{cases} f(\mathbf{x}) & \text{for regression,} \\ \text{sign}(f(\mathbf{x})) & \text{for binary classification,} \\ \arg \max_{j \in [k]} (f(\mathbf{x}))_j & \text{for multi-class classification,} \end{cases}$$

where $(f(\mathbf{x}))_j$ is the j -th element of $f(\mathbf{x})$. For regression problems, ℓ in (1) is often chosen as the *squared loss*

$$\ell_s(f(\mathbf{x}), y) = (\hat{y} - y)^2$$

for training and evaluation purposes. For classification problems, ℓ in (1) is often chosen as the *zero-one loss*

$$\ell_{01}(f(\mathbf{x}), y) = I(\hat{y} \neq y)$$

for evaluation, where I is the indicator function. However, since ℓ_{01} is discontinuous and therefore difficult to optimize, we often replace it with some *surrogate loss* [32, 33]. For example, ℓ_{01} is replaced by the *hinge loss*

$$\ell_h(f(\mathbf{x}), y) = \max(0, 1 - y f(\mathbf{x}))$$

for binary classification, and is replaced by the *softmax cross-entropy loss*

$$\begin{aligned}\ell_{\text{ce}}(f(\mathbf{x}), y) &= - \sum_{j=1}^k I(y = j) \log \left(\frac{\exp((f(\mathbf{x}))_j)}{\sum_{i=1}^k \exp((f(\mathbf{x}))_i)} \right) \\ &= \log \left(\sum_{i=1}^k \exp((f(\mathbf{x}))_i) \right) - (f(\mathbf{x}))_y\end{aligned}$$

for multi-class classification.

As the target domain density $p_{\text{te}}(\mathbf{x}, y)$ in (1) remains unknown, in supervised learning theories, it is commonly assumed that the training samples and test samples follow the same probability density, i.e., $p_{\text{tr}}(\mathbf{x}, y) = p_{\text{te}}(\mathbf{x}, y)$ [2, 3, 4, 5, 6, 7, 8]. With this assumption, *empirical risk minimization* (ERM) [4] is a common practice in supervised learning that learns a predictor f with training samples through the following procedures:

1. Choose a loss function $\ell(\cdot)$, so that the risk $R(f)$ is defined;
2. Choose a model \mathcal{F} , so that our goal is $\min_{f \in \mathcal{F}} R(f)$;
3. Approximate $R(f)$ by replacing the expectation by the sample average (under $p_{\text{tr}}(\mathbf{x}, y) = p_{\text{te}}(\mathbf{x}, y)$):

$$\widehat{R}(f) = \frac{1}{n_{\text{tr}}} \sum_{i=1}^{n_{\text{tr}}} [\ell(f(\mathbf{x}_i^{\text{tr}}), y_i^{\text{tr}})]; \quad (2)$$

4. Minimize the empirical risk $\widehat{R}(f)$, with appropriate regularization, by a favorite optimization algorithm:

$$\widehat{f} = \arg \min_{f \in \mathcal{F}} \widehat{R}(f). \quad (3)$$

ERM defines a family of learning algorithms and thanks to its mathematically clean formulation, it enables us to conduct theoretical analysis on the prediction performance. Indeed, the empirical risk estimator (2) is *unbiased* and the empirical risk minimizer (3) is *consistent*, i.e., \widehat{f} in (3) will converge to the optimal predictor $f^* = \arg \min_{f \in \mathcal{F}} R(f)$ as $n_{\text{tr}} \rightarrow \infty$ [4].

2.2 Transfer Learning

In many real-world problems, the training samples in the source domain and the test samples in the target domain are drawn from different densities, i.e., $p_{\text{tr}}(\mathbf{x}, y) \neq p_{\text{te}}(\mathbf{x}, y)$. In that case, ERM is not generally consistent anymore. Learning under such differing distributions is called *transfer learning* or *domain adaptation* [34, 15, 16, 35].

Due to various assumptions on how the joint distribution shifts from the source domain to the target domain, several transfer learning scenarios have been considered in the literature:

- *Covariate shift* is a traditional learning setting, which assumes that $p_{\text{tr}}(\mathbf{x}) \neq p_{\text{te}}(\mathbf{x})$ and $p_{\text{tr}}(y | \mathbf{x}) = p_{\text{te}}(y | \mathbf{x})$ [20, 23, 22, 16, 30, 31]. Even though $p(y | \mathbf{x})$ does not change, $p_{\text{tr}}(\mathbf{x}) \neq p_{\text{te}}(\mathbf{x})$ may break the consistency of ERM which occurs if the model \mathcal{F} is not expressive enough, so that fitting the training data does not fit the test data [20]. Covariate shift is a primal target in Sections 3, 4, and 5.

- *Output noise* is a common learning setting, where $p_{\text{tr}}(y | \mathbf{x}) \neq p_{\text{te}}(y | \mathbf{x})$ and $p_{\text{tr}}(\mathbf{x}) = p_{\text{te}}(\mathbf{x})$ which is opposite to covariate shift [36, 14]. In this scenario, we consider a label corruption process $p(\tilde{y} | y, \mathbf{x})$ where \tilde{y} denotes the corrupted label so that $p_{\text{tr}}(\tilde{y} | \mathbf{x}) = \sum_y p(\tilde{y} | y, \mathbf{x}) \cdot p_{\text{te}}(y | \mathbf{x})$, i.e., a label y may flip to every corrupted label $\tilde{y} \neq y$ with probability $p(\tilde{y} | y, \mathbf{x})$. Such output noise is extremely detrimental to ERM training, since an over-parameterized f is able to fit any training data even with random labels [37].
- *Class-prior/target shift* is also a frequently encountered setting in practice, where $p_{\text{tr}}(y) \neq p_{\text{te}}(y)$ while $p_{\text{tr}}(\mathbf{x} | y) = p_{\text{te}}(\mathbf{x} | y)$ [38, 39, 29, 40, 41, 42]. Under this shift, f will emphasize over-represented classes and neglect under-represented classes, which may raise fairness issues [43].
- *Class-conditional shift* refers to the setting that $p_{\text{tr}}(\mathbf{x} | y) \neq p_{\text{te}}(\mathbf{x} | y)$ and $p_{\text{tr}}(y) = p_{\text{te}}(y)$ [29]. Since the estimation of $p_{\text{te}}(\mathbf{x} | y)$ in this setting is in general ill-posed, a further assumption that there exists a transformation τ such that the conditional densities agree, i.e., $p_{\text{tr}}(\tau(\mathbf{x}) | y) = p_{\text{te}}(\tau(\mathbf{x}) | y)$, is often needed to solve the class-conditional shift problems [44, 45].
- *Full-distribution shift* is the most general setting where we consider $p_{\text{tr}}(\mathbf{x}, y) \neq p_{\text{te}}(\mathbf{x}, y)$ without any further information. The problem is extremely challenging and the use of validation data from the target domain is essential [46]. In principle, importance weighting is also applicable if validation data from the target domain is available. We discuss the details in Section 6.
- *Independent-component shift* also considers $p_{\text{tr}}(\mathbf{x}, y) \neq p_{\text{te}}(\mathbf{x}, y)$ but with an additional prior knowledge about the underlying generative mechanism. In particular, we consider the case where the distribution shift is attributed to a latent distribution shift of the *independent components* (ICs) and the mixing function to generate the data from the ICs is identical across the domains. We discuss this case in Section 7.

3 Importance Weighting for Covariate Shift Adaptation

In this section, we briefly introduce the *importance weighting* for covariate shift adaptation, including importance-weighted ERM and some representative approaches for direct importance estimation.

3.1 Importance-Weighted ERM

As discussed in Section 2, covariate shift may cause the failure of ERM. Importance weighting [15, 16, 20, 22] is a standard method for mitigating this problem. The essential idea of importance weighting under covariate shift is as follows:

$$\mathbb{E}_{(\mathbf{x}^{\text{te}}, y^{\text{te}}) \sim p_{\text{te}}(\mathbf{x}, y)} [\ell(f(\mathbf{x}^{\text{te}}), y^{\text{te}})] = \mathbb{E}_{(\mathbf{x}^{\text{tr}}, y^{\text{tr}}) \sim p_{\text{tr}}(\mathbf{x}, y)} [w(\mathbf{x}^{\text{tr}}) \ell(f(\mathbf{x}^{\text{tr}}), y^{\text{tr}})],$$

where $w(\mathbf{x}) = \frac{p_{\text{te}}(\mathbf{x})}{p_{\text{tr}}(\mathbf{x})}$ is referred to as the *importance*. This implies the expectation for any loss function $\ell(\cdot)$ over the test distribution is the importance-weighted expectation of the loss over the training distribution. This is how covariate shift is mitigated by importance weighting.

Importance-weighted ERM (IWERM) is accordingly defined as

$$\min_{f \in \mathcal{F}} \frac{1}{n_{\text{tr}}} \sum_{i=1}^{n_{\text{tr}}} [w(\mathbf{x}_i^{\text{tr}}) \ell(f(\mathbf{x}_i^{\text{tr}}), y_i^{\text{tr}})] . \quad (4)$$

For any fixed $f \in \mathcal{F}$, the importance weighted empirical risk is an unbiased estimator of the test risk and its minimizer is consistent [20].

3.2 Direct Importance Estimation

In the importance-weighted learning objective (4), the importance remains unknown. Next, we review approaches for directly estimating the importance $w(\mathbf{x})$. We assume that test input data $\{\mathbf{x}_j^{\text{te}}\}_{j=1}^{n_{\text{te}}}$ drawn independently from $p_{\text{te}}(\mathbf{x})$ are available for importance estimation, in addition to the training input data $\{\mathbf{x}_i^{\text{tr}}\}_{i=1}^{n_{\text{tr}}}$.

3.2.1 Kernel Mean Matching (KMM)

Kernel mean matching (KMM) [23] aims to find $w(\mathbf{x})$ that minimizes the mean discrepancy of nonlinear transformations of data drawn from p_{tr} and p_{te} in a *reproducing kernel Hilbert space* (RKHS), that is, for an RKHS \mathcal{H} ,

$$\begin{aligned} \min_{w(\mathbf{x})} & \left\| \mathbb{E}_{\mathbf{x}^{\text{te}} \sim p_{\text{te}}(\mathbf{x})} [K(\mathbf{x}^{\text{te}}, \cdot)] - \mathbb{E}_{\mathbf{x}^{\text{tr}} \sim p_{\text{tr}}(\mathbf{x})} [w(\mathbf{x}^{\text{tr}}) K(\mathbf{x}^{\text{tr}}, \cdot)] \right\|_{\mathcal{H}}^2 \\ \text{subject to} & \mathbb{E}_{\mathbf{x}^{\text{tr}} \sim p_{\text{tr}}(\mathbf{x})} [w(\mathbf{x}^{\text{tr}})] = 1 \text{ and } w(\mathbf{x}) \geq 0 \text{ for all } \mathbf{x} \in \mathcal{X}, \end{aligned}$$

where $\|\cdot\|_{\mathcal{H}}$ denotes the norm in \mathcal{H} and $K(\mathbf{x}, \mathbf{x}')$ is a kernel function [47]. An empirical version of the above optimization problem can be written as

$$\begin{aligned} \min_{\{w_i\}_{i=1}^{n_{\text{tr}}}} & \left[\frac{1}{2} \sum_{i,i'=1}^{n_{\text{tr}}} w_i w_{i'} K(\mathbf{x}_i^{\text{tr}}, \mathbf{x}_{i'}^{\text{tr}}) - \sum_{i=1}^{n_{\text{tr}}} w_i \kappa_i \right] \\ \text{subject to} & \frac{1}{n_{\text{tr}}} \left| \sum_{i=1}^{n_{\text{tr}}} w_i - n_{\text{tr}} \right| \leq \epsilon \text{ and } 0 \leq w_1, \dots, w_{n_{\text{tr}}} \leq B, \end{aligned}$$

where $\kappa_i = \frac{n_{\text{tr}}}{n_{\text{te}}} \sum_{j=1}^{n_{\text{te}}} K(\mathbf{x}_i^{\text{tr}}, \mathbf{x}_j^{\text{te}})$, and $B \geq 0$ and $\epsilon \geq 0$ are parameters for controlling the strength of regularization.

3.2.2 Least-Squares Importance Fitting (LSIF)

Least-squares importance fitting (LSIF) [26] adopts the squared loss for importance fitting. We model the importance $w(\mathbf{x})$ using a *linear-in-parameter model*:

$$g(\mathbf{x}) = \sum_{l=1}^b \beta_l \psi_l(\mathbf{x}) = \boldsymbol{\beta}^\top \boldsymbol{\psi}(\mathbf{x}),$$

where $\boldsymbol{\beta} = (\beta_1, \dots, \beta_b)^\top \in \mathbb{R}^b$ are the parameters to be learned,

$$\boldsymbol{\psi}(\mathbf{x}) = (\psi_1(\mathbf{x}), \dots, \psi_b(\mathbf{x}))^\top \in \mathbb{R}^b$$

is a vector of *basis functions*, and b denotes the number of basis functions. As basis functions, Gaussian kernels are practically useful [47], where $\psi_l(\mathbf{x}) := \exp(-\frac{\|\mathbf{x}-\mathbf{x}'\|^2}{2\sigma^2})$ for some $\mathbf{x}' \in \mathbb{R}^{d_{\text{in}}}$ and $\sigma > 0$. The parameters $\boldsymbol{\beta}$ in $g(\mathbf{x})$ are determined by minimizing the following squared-error J :

$$\begin{aligned} J(\boldsymbol{\beta}) &= \frac{1}{2} \mathbb{E}_{\mathbf{x}^{\text{tr}} \sim p_{\text{tr}}(\mathbf{x})} \left[(g(\mathbf{x}^{\text{tr}}) - w(\mathbf{x}^{\text{tr}}))^2 \right] \\ &= \frac{1}{2} \mathbb{E}_{\mathbf{x}^{\text{tr}} \sim p_{\text{tr}}(\mathbf{x})} \left[g^2(\mathbf{x}^{\text{tr}}) \right] - \mathbb{E}_{\mathbf{x}^{\text{tr}} \sim p_{\text{tr}}(\mathbf{x})} \left[g(\mathbf{x}^{\text{tr}}) w(\mathbf{x}^{\text{tr}}) \right] + \frac{1}{2} \mathbb{E}_{\mathbf{x}^{\text{tr}} \sim p_{\text{tr}}(\mathbf{x})} \left[w^2(\mathbf{x}^{\text{tr}}) \right], \\ &= \underbrace{\frac{1}{2} \mathbb{E}_{\mathbf{x}^{\text{tr}} \sim p_{\text{tr}}(\mathbf{x})} \left[g^2(\mathbf{x}^{\text{tr}}) \right] - \mathbb{E}_{\mathbf{x}^{\text{te}} \sim p_{\text{te}}(\mathbf{x})} \left[g(\mathbf{x}^{\text{te}}) \right]}_{:=J'(\boldsymbol{\beta})} + \underbrace{\frac{1}{2} \mathbb{E}_{\mathbf{x}^{\text{tr}} \sim p_{\text{tr}}(\mathbf{x})} \left[w^2(\mathbf{x}^{\text{tr}}) \right]}_{:=C}. \end{aligned} \quad (5)$$

The last term C is a constant with respect to $\boldsymbol{\beta}$ and thus it can be safely ignored. Approximating the expectations in $J'(\boldsymbol{\beta})$, we have

$$\begin{aligned} \hat{J}'(\boldsymbol{\beta}) &= \frac{1}{2n_{\text{tr}}} \sum_{i=1}^{n_{\text{tr}}} g^2(\mathbf{x}_i^{\text{tr}}) - \frac{1}{n_{\text{te}}} \sum_{j=1}^{n_{\text{te}}} g(\mathbf{x}_j^{\text{te}}) \\ &= \frac{1}{2} \sum_{l,l'=1}^b \beta_l \beta_{l'} \left(\frac{1}{n_{\text{tr}}} \sum_{i=1}^{n_{\text{tr}}} \psi_l(\mathbf{x}_i^{\text{tr}}) \psi_{l'}(\mathbf{x}_i^{\text{tr}}) \right) - \sum_{l=1}^b \beta_l \left(\frac{1}{n_{\text{te}}} \sum_{j=1}^{n_{\text{te}}} \psi_l(\mathbf{x}_j^{\text{te}}) \right) \\ &= \frac{1}{2} \boldsymbol{\beta}^\top \hat{\mathbf{H}} \boldsymbol{\beta} - \hat{\mathbf{h}}^\top \boldsymbol{\beta}, \end{aligned}$$

where the (l, l') -th element of $\hat{\mathbf{H}}$ is $\frac{1}{n_{\text{tr}}} \sum_{i=1}^{n_{\text{tr}}} \psi_l(\mathbf{x}_i^{\text{tr}}) \psi_{l'}(\mathbf{x}_i^{\text{tr}})$ and l -th element of $\hat{\mathbf{h}}$ is $\frac{1}{n_{\text{te}}} \sum_{j=1}^{n_{\text{te}}} \psi_l(\mathbf{x}_j^{\text{te}})$.

Since the importance $w(\mathbf{x})$ is non-negative by definition, we may practically solve the following optimization problem:

$$\min_{\boldsymbol{\beta}} \left[\frac{1}{2} \boldsymbol{\beta}^\top \hat{\mathbf{H}} \boldsymbol{\beta} - \hat{\mathbf{h}}^\top \boldsymbol{\beta} + \lambda \mathbf{1}_b^\top \boldsymbol{\beta} \right] \text{ subject to } \boldsymbol{\beta} \geq \mathbf{0}_b, \quad (6)$$

where $\mathbf{1}_b$ and $\mathbf{0}_b$ are the b -dimensional vectors with all ones and zeros. $\boldsymbol{\beta} \geq \mathbf{0}_b$ is applied in the element-wise manner. The term $\lambda \mathbf{1}_b^\top \boldsymbol{\beta}$ is for regularization and a non-negative λ is the parameter controlling the regularization effect. Note that (6) is a convex quadratic programming problem and the unique global optimal solution can be obtained by using some standard optimization packages.

Unconstrained LSIF (uLSIF) [26] is an approximation method for LSIF by removing the non-negativity constraint in (6). This leads to the following unconstrained optimization problem:

$$\min_{\boldsymbol{\beta} \in \mathbb{R}^b} \left[\frac{1}{2} \boldsymbol{\beta}^\top \hat{\mathbf{H}} \boldsymbol{\beta} - \hat{\mathbf{h}}^\top \boldsymbol{\beta} + \frac{\lambda}{2} \boldsymbol{\beta}^\top \boldsymbol{\beta} \right].$$

Here $\frac{\lambda}{2} \boldsymbol{\beta}^\top \boldsymbol{\beta}$ is introduced for regularization rather than $\lambda \mathbf{1}_b^\top \boldsymbol{\beta}$ because the linear term does not work as a regularizer without the nonnegativity constraint. The solution can be analytically computed as $\tilde{\boldsymbol{\beta}} = (\hat{\mathbf{H}} + \lambda \mathbf{I}_b)^{-1} \hat{\mathbf{h}}$, where \mathbf{I}_b is the b -dimensional identity matrix.

To compensate for the approximation error that some of the learned β can be negative, the solution is modified as $\hat{\beta} = \max(\mathbf{0}_b, \tilde{\beta})$, where the max operation is applied in the element-wise manner for a pair of vectors.

4 Adaptive Importance Weighting for Covariate Shift Adaptation

Although IWERM gives a consistent predictor as shown in Section 3, it can also produce an unstable predictor due to high variance of the importance weights for the training samples, which indicates that IWERM may not be the best method in the finite-sample case [20]. Therefore, in practice, it is preferable to slightly stabilize IWERM during training. In this section, we introduce two such adaptive methods for covariate shift adaptation.

4.1 Exponentially-flattened IWERM (EIWERM)

The first method flattening the importance weights in IWERM is *exponentially-flattened IWERM* (EIWERM) [20]:

$$\min_{f \in \mathcal{F}} \frac{1}{n_{\text{tr}}} \sum_{i=1}^{n_{\text{tr}}} \left[(w(\mathbf{x}_i^{\text{tr}}))^{\gamma} \ell(f(\mathbf{x}_i^{\text{tr}}), y_i^{\text{tr}}) \right],$$

where γ ($0 \leq \gamma \leq 1$) is called the *flattening parameter*.

The flattening parameter controls stability and consistency of the predictor: $\gamma = 0$ corresponds to ordinary ERM (the uniform weight, which yields a stable but inconsistent predictor), and $\gamma = 1$ corresponds to IWERM (the importance weight, which yields a consistent but unstable predictor). An intermediate value of γ would provide the optimal control of the trade-off between stability and consistency.

4.2 Relative IWERM (RIWERM)

A potential drawback of EIWERM when the importance $w(\mathbf{x})$ is replaced with an estimate $\hat{w}(\mathbf{x})$ — its exponent $(\hat{w}(\mathbf{x}))^{\gamma}$ is not necessarily a good estimate of the original exponent $(w(\mathbf{x}))^{\gamma}$. Indeed, estimation of $(w(\mathbf{x}))^{\gamma}$ may be hard/easy if γ is large/small, since the target function $(w(\mathbf{x}))^{\gamma}$ is more/less fluctuated. To cope with this problem, *relative IWERM* (RIWERM) [27] was proposed which learned a flattened importance weight directly. More specifically, it estimates the η -relative importance weight $w_{\eta}(\mathbf{x})$ ($0 \leq \eta \leq 1$) defined as

$$w_{\eta}(\mathbf{x}) := \frac{p_{\text{te}}(\mathbf{x})}{\eta p_{\text{te}}(\mathbf{x}) + (1 - \eta) p_{\text{tr}}(\mathbf{x})}.$$

Consequently, RIWERM minimizes the following weighted loss in the same way as uLSIF:

$$\min_{f \in \mathcal{F}} \frac{1}{n_{\text{tr}}} \sum_{i=1}^{n_{\text{tr}}} \left[w_{\eta}(\mathbf{x}_i^{\text{tr}}) \ell(f(\mathbf{x}_i^{\text{tr}}), y_i^{\text{tr}}) \right].$$

Similarly to the role of flattening parameter γ in EIWERM, the parameter η also controls stability and consistency of the predictor: $\eta = 0$ corresponds to IWERM and $\eta = 1$ corresponds to the ordinary ERM.

To estimate the relative importance $w_\eta(\mathbf{x})$, *relative uLSIF* (RuLSIF) was proposed and it learns a relative importance model $g_\eta(\mathbf{x})$ by minimizing the following expected squared-error J_η :

$$\begin{aligned} J_\eta(g_\eta) &= \frac{1}{2} \mathbb{E}_{\eta p_{\text{te}}(\mathbf{x}) + (1-\eta) p_{\text{tr}}(\mathbf{x})} [(g_\eta(\mathbf{x}) - w_\eta(\mathbf{x}))^2] \\ &= \frac{\eta}{2} \mathbb{E}_{p_{\text{te}}(\mathbf{x})} [g_\eta^2(\mathbf{x})] + \frac{1-\eta}{2} \mathbb{E}_{p_{\text{tr}}(\mathbf{x})} [g_\eta^2(\mathbf{x})] - \mathbb{E}_{p_{\text{te}}(\mathbf{x})} [g_\eta(\mathbf{x})] + \text{Const.} \end{aligned}$$

The analytical solution minimizing the empirical version of the objective J_η can be obtained similarly to uLSIF (see Section 3.2.2) when the linear-in-parameter model is used and the details can be found in [27].

5 Upper Bound Minimization for Covariate Shift Adaptation

As we have seen in Sections 3 and 4, covariate shift adaptation methods usually need an intermediate step for estimating the importance. A natural question is whether we can have a more direct way to solve the covariate shift adaptation problem. In this section, we answer it affirmatively by introducing a one-step approach for covariate shift adaptation [30, 31] which integrates the importance estimation step and the importance-weighted ERM step by minimizing an upper bound of the test risk.

5.1 One-step Approach

First, we derive an upper bound of the test risk (1), which is the key of the one-step approach.

Theorem 1. [30] *Let $w(\mathbf{x})$ be the importance $p_{\text{te}}(\mathbf{x})/p_{\text{tr}}(\mathbf{x})$ and $\mathcal{F} \subseteq \{f: \mathcal{X} \rightarrow \mathbb{R}\}$ be a given hypothesis set. Suppose that there is a constant $m \in \mathbb{R}$ such that $\ell(f(\mathbf{x}), y) \leq m$ holds for every $f \in \mathcal{F}$ and every $(\mathbf{x}, y) \in \mathcal{X} \times \mathcal{Y}$. Then, for any $f \in \mathcal{F}$ and any measurable function $g: \mathcal{X} \rightarrow \mathbb{R}$, the test risk is bounded as follows under covariate shift:*

$$\begin{aligned} \frac{1}{2} R^2(f) \leq J(f, g) &:= (\mathbb{E}_{(\mathbf{x}^{\text{tr}}, y^{\text{tr}}) \sim p_{\text{tr}}(\mathbf{x}, y)} [g(\mathbf{x}^{\text{tr}}) \ell(f(\mathbf{x}^{\text{tr}}), y^{\text{tr}})])^2 \\ &\quad + m^2 \mathbb{E}_{\mathbf{x}^{\text{tr}} \sim p_{\text{tr}}(\mathbf{x})} [(g(\mathbf{x}^{\text{tr}}) - w(\mathbf{x}^{\text{tr}}))^2]. \end{aligned} \quad (7)$$

Furthermore, if g is non-negative and ℓ_{UB} bounds ℓ from above, we have

$$\begin{aligned} J(f, g) \leq J_{\text{UB}}(f, g) &:= (\mathbb{E}_{(\mathbf{x}^{\text{tr}}, y^{\text{tr}}) \sim p_{\text{tr}}(\mathbf{x}, y)} [g(\mathbf{x}^{\text{tr}}) \ell_{\text{UB}}(f(\mathbf{x}^{\text{tr}}), y^{\text{tr}})])^2 \\ &\quad + m^2 \mathbb{E}_{\mathbf{x}^{\text{tr}} \sim p_{\text{tr}}(\mathbf{x})} [(g(\mathbf{x}^{\text{tr}}) - w(\mathbf{x}^{\text{tr}}))^2]. \end{aligned} \quad (8)$$

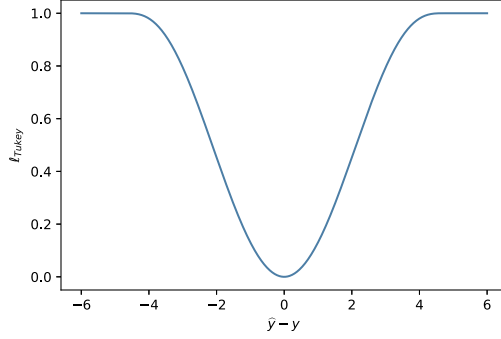


Figure 1: Tukey's loss defined as $\ell_{\text{Tukey}}(\hat{y}, y) := \min \left(1 - \left[1 - (\hat{y} - y)^2 / \rho^2 \right]^3, 1 \right) \leq 1$. It has been widely used in the context of robust statistics. The hyper-parameter $\rho > 0$ is usually set to 4.685 for this loss function, and it provides an asymptotic efficiency 95% of that of least squares for Gaussian noise [49]. Here, we rescale the standard Tukey's bisquare loss for convenience, which does not change the minimizer of the test risk.

Proof. According to the Cauchy-Schwarz inequality, we have

$$\begin{aligned}
\frac{1}{2} R^2(f) &= \frac{1}{2} \left(\mathbb{E}_{p_{\text{tr}}(\mathbf{x}, y)} \left[w(\mathbf{x}^{\text{tr}}) \ell(f(\mathbf{x}^{\text{tr}}), y^{\text{tr}}) \right] \right)^2 \\
&\leq \left(\mathbb{E}_{p_{\text{tr}}(\mathbf{x}, y)} \left[g(\mathbf{x}^{\text{tr}}) \ell(f(\mathbf{x}^{\text{tr}}), y^{\text{tr}}) \right] \right)^2 \\
&\quad + \left(\mathbb{E}_{p_{\text{tr}}(\mathbf{x}, y)} \left[(w(\mathbf{x}^{\text{tr}}) - g(\mathbf{x}^{\text{tr}})) \ell(f(\mathbf{x}^{\text{tr}}), y^{\text{tr}}) \right] \right)^2 \\
&\leq \left(\mathbb{E}_{p_{\text{tr}}(\mathbf{x}, y)} \left[g(\mathbf{x}^{\text{tr}}) \ell(f(\mathbf{x}^{\text{tr}}), y^{\text{tr}}) \right] \right)^2 \\
&\quad + \mathbb{E}_{p_{\text{tr}}(\mathbf{x})} \left[(g(\mathbf{x}^{\text{tr}}) - w(\mathbf{x}^{\text{tr}}))^2 \right] \mathbb{E}_{p_{\text{tr}}(\mathbf{x}, y)} \left[\ell^2(f(\mathbf{x}^{\text{tr}}), y^{\text{tr}}) \right] \\
&\leq \left(\mathbb{E}_{p_{\text{tr}}(\mathbf{x}, y)} \left[g(\mathbf{x}^{\text{tr}}) \ell(f(\mathbf{x}^{\text{tr}}), y^{\text{tr}}) \right] \right)^2 + m^2 \mathbb{E}_{p_{\text{tr}}(\mathbf{x})} \left[(g(\mathbf{x}^{\text{tr}}) - w(\mathbf{x}^{\text{tr}}))^2 \right],
\end{aligned}$$

This proves (7), and based on this, (8) is obvious. \square

For classification problems, the test risk $R(f)$ is typically defined by the zero-one loss, and thus the boundedness assumption of the loss function in Theorem 1 holds with $m = 1$. For regression problems, the squared loss is a typical choice, but it violates the boundedness assumption. Instead, we define $R(f)$ using Tukey's bisquare loss [48] (see Fig. 1).

Remark: The two-step approach that first applies uLSIF to estimate the importance weights and then employs IWERM with the estimated importance is equivalent to minimizing the second term of the above upper bounds first and then minimizing the first term, which leads to a sub-optimal solution to the upper-bound minimization.

Instead of estimating the unknown $w(\mathbf{x})$ for minimizing $R(f)$ as in the previous two-step approaches, we propose a one-step approach that minimizes the upper bound $J(f, g)$ or $J_{\text{UB}}(f, g)$ based on Theorem 1.

For classification problems, $J(f, g)$ is defined using the zero-one loss, with which training will not be tractable [32]. Fortunately, the latter part of Theorem 1 allows us to minimize $J_{\text{UB}}(f, g)$ instead, with ℓ_{UB} being any (sub-)differentiable approximation that bounds the zero-one loss from above so that we can apply any gradient method such as stochastic gradient descent [50]. Examples of such ℓ_{UB} include the hinge loss and the squared loss in binary classification and the softmax cross-entropy loss in multi-class classification. For regression problems, Tukey’s loss is already sub-differentiable, but we can use the squared loss that bounds Tukey’s loss which makes the optimization problem simpler as described later. This is again justified by Theorem 1 with the squared loss used as the upper-bounding loss ℓ_{UB} .

Although the second expectation in $J_{\text{UB}}(f, g)$ contains an unknown term $w(\mathbf{x})$, it can be estimated from the samples on hand, up to addition by a constant C as shown in (5). Since the true distributions are unknown, we minimize its empirical version $\widehat{J}_{\text{UB}}(f, g)$ with respect to f and non-negative g in some given hypothesis sets \mathcal{F} and \mathcal{G}_+ :

$$\begin{aligned} \widehat{J}_{\text{UB}}(f, g; S) := & \left(\frac{1}{n_{\text{tr}}} \sum_{i=1}^{n_{\text{tr}}} g(\mathbf{x}_i^{\text{tr}}) \ell_{\text{UB}}(f(\mathbf{x}_i^{\text{tr}}), y_i^{\text{tr}}) \right)^2 \\ & + m^2 \left(\frac{1}{n_{\text{tr}}} \sum_{i=1}^{n_{\text{tr}}} g^2(\mathbf{x}_i^{\text{tr}}) - \frac{2}{n_{\text{te}}} \sum_{j=1}^{n_{\text{te}}} g(\mathbf{x}_j^{\text{te}}) + C \right), \end{aligned} \quad (9)$$

where $S := \{(\mathbf{x}_i^{\text{tr}}, y_i^{\text{tr}})\}_{i=1}^{n_{\text{tr}}} \cup \{\mathbf{x}_j^{\text{te}}\}_{j=1}^{n_{\text{te}}}$ is the set of sample points. Notice that constant C can be safely ignored in the minimization.

In Algorithm 1, we present an alternating minimization algorithm that can be employed when $f(\mathbf{x})$ and $g(\mathbf{x})$ are linear-in-parameter models used in Section 3.2.2, i.e.,

$$f(\mathbf{x}) = \boldsymbol{\alpha}^\top \boldsymbol{\phi}(\mathbf{x}) \quad \text{and} \quad g(\mathbf{x}) = \boldsymbol{\beta}^\top \boldsymbol{\psi}(\mathbf{x}), \quad (10)$$

where $\boldsymbol{\alpha} \in \mathbb{R}^{b_f}$ and $\boldsymbol{\beta} \in \mathbb{R}^{b_g}$ are parameters, and $\boldsymbol{\phi}$ and $\boldsymbol{\psi}$ are b_f -dimensional and b_g -dimensional vectors of basis functions.

First, we minimize the objective (9) with respect to g while fixing f . This step has an analytic solution as shown in Algorithm 1, Line 6, where $\boldsymbol{\Phi}_{\text{tr}} = (\boldsymbol{\phi}(\mathbf{x}_1^{\text{tr}}), \dots, \boldsymbol{\phi}(\mathbf{x}_{n_{\text{tr}}}^{\text{tr}}))^\top$, $\boldsymbol{\Psi}_{\text{tr}} = (\boldsymbol{\psi}(\mathbf{x}_1^{\text{tr}}), \dots, \boldsymbol{\psi}(\mathbf{x}_{n_{\text{tr}}}^{\text{tr}}))^\top$, $\boldsymbol{\Psi}_{\text{te}} = (\boldsymbol{\psi}(\mathbf{x}_1^{\text{te}}), \dots, \boldsymbol{\psi}(\mathbf{x}_{n_{\text{te}}}^{\text{te}}))^\top$, $\mathbf{1} = (1, \dots, 1)^\top$, and \mathbf{I} is the identity matrix.

Next, we minimize the objective (9) with respect to f while fixing g . In this step, we can safely ignore the second term and remove the square operation of the first term in the objective (9) to reduce the problem into weighted empirical risk minimization (cf. Algorithm 1, Line 12) by forcing g to be non-negative with a rounding up technique [26] as shown in Algorithm 1, Line 7. For regression problems, the method of iteratively reweighted least squares (IRLS) [48] can be used for optimizing Tukey’s bisquare loss. In practice, we suggest using the squared loss as a convex approximation of Tukey’s loss to obtain a closed-form solution as shown in Algorithm 1, Line 10 for reducing computation time, and we compare their performance in the experiments. For classification with linear-in-parameter models using the hinge loss, then the weighted support vector machine [51] can be used. After this step, we go back to the step for updating g and repeat the procedure.

On the other hand, when $f(\mathbf{x})$ and $g(\mathbf{x})$ are modeled as neural networks, we present a gradient-based alternating minimization algorithm described in Algorithm 2 that is more convenient for training neural networks.

Algorithm 1 Alternating Minimization with Linear-in-parameter Models

- 1: $\alpha_0 \leftarrow$ an arbitrary b_f -dimensional vector
 - 2: $\lambda \leftarrow$ a positive ℓ_2 -regularization parameter
 - 3: $\mu \leftarrow$ a positive ℓ_2 -regularization parameter
 - 4: **for** $t = 0, 1, \dots, T - 1$ **do**
 - 5: $\mathbf{l}_t \leftarrow (\ell_{\text{UB}}(\alpha_t^\top \phi(\mathbf{x}_1^{\text{tr}}), y_1^{\text{tr}}), \dots, \ell_{\text{UB}}(\alpha_t^\top \phi(\mathbf{x}_{n_{\text{tr}}}^{\text{tr}}), y_{n_{\text{tr}}}^{\text{tr}}))^\top$
 - 6: $\beta_{t+1} \leftarrow \left(\frac{1}{n_{\text{tr}}} \Psi_{\text{tr}}^\top \Psi_{\text{tr}} + \frac{1}{m^2 n_{\text{tr}}^2} \Psi_{\text{tr}}^\top \mathbf{l}_t \mathbf{l}_t^\top \Psi_{\text{tr}} + \frac{1}{m^2} \lambda \mathbf{I} \right)^{-1} \frac{1}{n_{\text{te}}} \Psi_{\text{te}}^\top \mathbf{1}$
 - 7: $\beta_{t+1} \leftarrow \max(\beta_{t+1}, \mathbf{0})$
 - 8: $w_i^{t+1} \leftarrow \beta_{t+1}^\top \psi(\mathbf{x}_i^{\text{tr}}), i = 1, \dots, n_{\text{tr}}$
 - 9: **if** ℓ_{UB} is the squared loss **then**
 - 10: $\alpha_{t+1} \leftarrow (\Phi_{\text{tr}}^\top \mathbf{W}_{t+1} \Phi_{\text{tr}} + \mu n_{\text{tr}} \mathbf{I})^{-1} \Phi_{\text{tr}}^\top \mathbf{W}_{t+1} \mathbf{y}_{\text{tr}},$
 where $\mathbf{W}_{t+1} = \text{diag}(w_1^{t+1}, \dots, w_{n_{\text{tr}}}^{t+1})$ and $\mathbf{y}_{\text{tr}} = (y_1^{\text{tr}}, \dots, y_{n_{\text{tr}}}^{\text{tr}})^\top$
 - 11: **else**
 - 12: $\alpha_{t+1} \leftarrow \arg \min_{\alpha} \frac{1}{n_{\text{tr}}} \sum_{i=1}^{n_{\text{tr}}} w_i^{t+1} \ell_{\text{UB}}(\alpha^\top \phi(\mathbf{x}_i^{\text{tr}}), y_i^{\text{tr}}) + \mu \alpha^\top \alpha$
 - 13: **end if**
 - 14: **end for**
-

5.2 Theoretical Analysis

In what follows, we establish a generalization error bound for the proposed method in terms of the *Rademacher complexity* [52] in regression and binary classification. Due to the space limitation, we omit the proofs here — they can be found in [30, 31].

Lemma 2. Assume that (a) there exist some constants $M \geq m$ and $L > 0$ such that $\ell_{\text{UB}}(f(\mathbf{x}), y) \leq M$ holds for every $f \in \mathcal{F}$ and every $(\mathbf{x}, y) \in \mathcal{X} \times \mathcal{Y}$ and $y \mapsto \ell_{\text{UB}}(y, y')$ is L -Lipschitz for every fixed $y' \in \mathcal{Y}$;¹ (b) there exists some constant $G \geq 1$ such that $g(\mathbf{x}) \leq G$ for every $g \in \mathcal{G}_+$ and every $\mathbf{x} \in \mathcal{X}$. Let $\mathcal{G} = \mathcal{G}_+ \cup -\mathcal{G}_+$. Then for any $\delta > 0$, with probability at least $1 - \delta$ over the draw of S , the following holds for all $f \in \mathcal{F}, g \in \mathcal{G}_+$ uniformly:

$$\begin{aligned} J_{\text{UB}}(f, g) &\leq \widehat{J}_{\text{UB}}(f, g; S) + 8MG(M + G)(L\mathfrak{R}_{n_{\text{tr}}}^{\text{tr}}(\mathcal{F}) + \mathfrak{R}_{n_{\text{tr}}}^{\text{tr}}(\mathcal{G})) \\ &\quad + 4M^2\mathfrak{R}_{n_{\text{te}}}^{\text{te}}(\mathcal{G}) + 5M^2G^2\sqrt{\frac{\log \frac{1}{\delta}}{2}} \left(\frac{1}{\sqrt{n_{\text{tr}}}} + \frac{1}{\sqrt{n_{\text{te}}}} \right), \end{aligned} \quad (11)$$

where $\mathfrak{R}_{n_{\text{tr}}}^{\text{tr}}(\mathcal{F})$ and $\mathfrak{R}_{n_{\text{tr}}}^{\text{tr}}(\mathcal{G})$ are the Rademacher complexities of \mathcal{F} and \mathcal{G} , respectively, for the sampling of size n_{tr} from $p_{\text{tr}}(\mathbf{x})$, and $\mathfrak{R}_{n_{\text{te}}}^{\text{te}}(\mathcal{G})$ is the Rademacher complexity of \mathcal{G} for the sampling of size n_{te} from $p_{\text{te}}(\mathbf{x})$.

Combining (7), (8), and (11), we obtain the following theorem.

Theorem 3. Suppose that the assumptions in Lemma 2 hold. Then, for any $\delta > 0$, with probability at least $1 - \delta$ over the draw of S , the test risk can be bounded as follows for all

¹This assumption is valid when $\sup_{f \in \mathcal{F}} \|f\|_\infty$ and $\sup_{y \in \mathcal{Y}} |y|$ are bounded.

Algorithm 2 Gradient-based Alternating Minimization

```

1:  $\mathcal{D}^{\text{tr}}, \mathcal{D}_{\text{in}}^{\text{te}} \leftarrow \{(\mathbf{x}_i^{\text{tr}}, y_i^{\text{tr}})\}_{i=1}^{n_{\text{tr}}}, \{\mathbf{x}_j^{\text{te}}\}_{j=1}^{n_{\text{te}}}$ 
2:  $\mathcal{A} \leftarrow$  a gradient-based optimizer
3:  $f \leftarrow$  an arbitrary classifier
4: for round = 0, 1, ..., numOfRounds - 1 do
5:   for epoch = 0, 1, ..., numOfEpochsForG - 1 do
6:     for  $k = 0, 1, \dots, \text{numOfMiniBatches} - 1$  do
7:        $\mathcal{D}_k^{\text{tr}}, \mathcal{D}_{\text{in},k}^{\text{te}} \leftarrow \text{sampleMiniBatch}(\mathcal{D}^{\text{tr}}, \mathcal{D}_{\text{in}}^{\text{te}})$ 
8:        $g \leftarrow \mathcal{A}(g, \nabla_g \widehat{J}_{\text{UB}}(f, g; \mathcal{D}_k^{\text{tr}} \cup \mathcal{D}_{\text{in},k}^{\text{te}}))$ 
9:     end for
10:   end for
11:   for epoch = 0, 1, ..., numOfEpochsForF - 1 do
12:     for  $k = 0, 1, \dots, \text{numOfMiniBatches} - 1$  do
13:        $\mathcal{D}_k^{\text{tr}} \leftarrow \text{sampleMiniBatch}(\mathcal{D}^{\text{tr}})$ 
14:        $w_i \leftarrow \max(g(\mathbf{x}_i), 0), \forall (\mathbf{x}_i, \cdot) \in \mathcal{D}_k^{\text{tr}}$ 
15:        $w_i \leftarrow w_i / \sum_j w_j, \forall i$ 
16:        $L_k \leftarrow \sum_{(\mathbf{x}_i, y_i) \in \mathcal{D}_k^{\text{tr}}} w_i \ell_{\text{UB}}(f(\mathbf{x}_i), y_i)$ 
17:        $f \leftarrow \mathcal{A}(f, \nabla_f L_k)$ 
18:     end for
19:   end for
20: end for

```

$f \in \mathcal{F}$ uniformly:

$$\begin{aligned}
\frac{1}{2} R^2(f) &\leq \min_{g \in \mathcal{G}_+} \widehat{J}_{\text{UB}}(f, g; S) + 8MG(M+G)(L\mathfrak{R}_{n_{\text{tr}}}^{\text{tr}}(\mathcal{F}) + \mathfrak{R}_{n_{\text{tr}}}^{\text{tr}}(\mathcal{G})) \\
&\quad + 4M^2\mathfrak{R}_{n_{\text{te}}}^{\text{te}}(\mathcal{G}) + 5M^2G^2\sqrt{\frac{\log \frac{1}{\delta}}{2}} \left(\frac{1}{\sqrt{n_{\text{tr}}}} + \frac{1}{\sqrt{n_{\text{te}}}} \right).
\end{aligned}$$

Theorem 3 implies that minimizing $\widehat{J}_{\text{UB}}(f, g)$, as the proposed method does, amounts to minimizing an upper bound of the test risk. Furthermore, the following theorem shows a generalization error bound for the minimizer obtained by the proposed method.

Theorem 4. Let $(\widehat{f}, \widehat{g}) = \arg \min_{(f, g) \in \mathcal{F} \times \mathcal{G}_+} \widehat{J}_{\text{UB}}(f, g)$. Then, under the assumptions of Lemma 2, for any $\delta > 0$, it holds with probability at least $1 - \delta$ over the draw of S that

$$\begin{aligned}
\frac{1}{2} R^2(\widehat{f}) &\leq \min_{f \in \mathcal{F}, g \in \mathcal{G}_+} J_{\text{UB}}(f, g) + 8MG(M+G)(L\mathfrak{R}_{n_{\text{tr}}}^{\text{tr}}(\mathcal{F}) + \mathfrak{R}_{n_{\text{tr}}}^{\text{tr}}(\mathcal{G})) \\
&\quad + 4M^2\mathfrak{R}_{n_{\text{te}}}^{\text{te}}(\mathcal{G}) + 10M^2G^2\sqrt{\frac{\log \frac{1}{\delta}}{2}} \left(\frac{1}{\sqrt{n_{\text{tr}}}} + \frac{1}{\sqrt{n_{\text{te}}}} \right) + \frac{M^2G^2}{n_{\text{tr}}}.
\end{aligned}$$

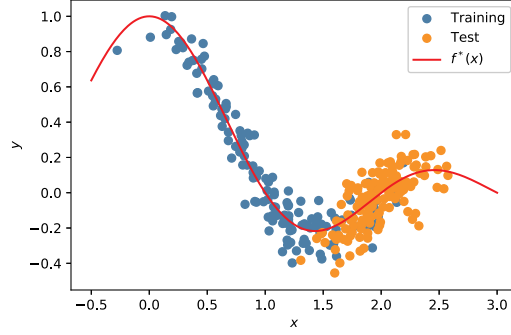


Figure 2: A toy regression example. The training input points (blue) are distributed on the left-hand side of the input domain and the test input points (orange) are distributed on the right-hand side. The two distributions share the same regression function f^* (the red curve).

If we use linear-in-parameter models with bounded norms, then $\mathfrak{R}_{n_{\text{tr}}}^{\text{tr}}(\mathcal{F}) = O(1/\sqrt{n_{\text{tr}}})$, $\mathfrak{R}_{n_{\text{tr}}}^{\text{tr}}(\mathcal{G}) = O(1/\sqrt{n_{\text{tr}}})$, and $\mathfrak{R}_{n_{\text{te}}}^{\text{te}}(\mathcal{G}) = O(1/\sqrt{n_{\text{te}}})$ [53, 54]. Furthermore, if we assume that the approximation error of \mathcal{G}_+ is zero, i.e., $r \in \mathcal{G}_+$, then $\min_{f \in \mathcal{F}, g \in \mathcal{G}_+} J_{\text{UB}}(f, g) \leq J_{\text{UB}}(f^*, r) = R_{\text{UB}}^2(f^*)$, where R_{UB} is the test risk defined with ℓ_{UB} and $f^* = \arg \min_{f \in \mathcal{F}} R_{\text{UB}}(f)$. Thus,

$$R(\hat{f}) \leq \sqrt{2}R_{\text{UB}}(f^*) + O_p(1/\sqrt[4]{n_{\text{tr}}} + 1/\sqrt[4]{n_{\text{te}}}).$$

When the best-in-class test risk $R_{\text{UB}}(f^*)$ is small, this bound would theoretically guarantee a good performance of the proposed method.

5.3 Experiments

In this section, we examine the effectiveness of the proposed method via a toy illustration and experiments on regression and classification benchmark datasets.

5.3.1 Illustration with Toy Regression Datasets

First, we report the results of experiments on a toy regression dataset.

Let us consider a one-dimensional regression problem. Let the training and test input densities be

$$p_{\text{tr}}(x) = N(x; 1, (0.5)^2) \quad \text{and} \quad p_{\text{te}}(x) = N(x; 2, (0.25)^2),$$

where $N(x; \mu, \sigma^2)$ denotes the Gaussian density with mean μ and variance σ^2 . Consider the case where the output labels of examples are generated by

$$y = f^*(x) + \epsilon \quad \text{with} \quad f^*(x) = \text{sinc}(x),$$

and the noise ϵ following $N(0, (0.1)^2)$ is independent of x . As illustrated in Fig. 2, the training input points are distributed on the left-hand side of the input domain and the test input points are distributed on the right-hand side. We sampled $n_{\text{tr}} = 150$ labeled i.i.d. training samples $\{(x_i^{\text{tr}}, y_i^{\text{tr}})\}_{i=1}^{n_{\text{tr}}}$ with each x_i^{tr} following $p_{\text{tr}}(x)$ and $n_{\text{te}} = 150$ unlabeled i.i.d. test samples $\{x_j^{\text{te}}\}_{j=1}^{n_{\text{te}}}$ following $p_{\text{te}}(x)$ for learning the target function $f^*(x)$ in the experiment.

Table 1: Mean squared test errors averaged over 100 trials on the toy dataset. The numbers in the brackets are the standard deviations. The best method and comparable ones based on the *paired t-test* at the significance level 5% are described in bold face. The computation time is averaged over 100 trials. “Squared” denotes the squared loss, while “Tukey” denotes Tukey’s bisquare loss.

Methods	MSE(SD)	Computation time (sec)
ERM (squared)	0.1453 (0.1812)	0.04
ERM (Tukey)	0.0760 (0.0733)	0.09
EIWERM (squared)	0.0198 (0.0151)	0.33
EIWERM (Tukey)	0.0161 (0.0106)	0.76
RIWERM (squared)	0.0162 (0.0100)	0.47
RIWERM (Tukey)	0.0149 (0.0073)	0.84
one-step (squared)	0.0131 (0.0036)	0.73
one-step (Tukey)	0.0125 (0.0021)	1.50

We compared our one-step approach with three baseline methods, which are the ordinary ERM, EIWERM with uLSIF, and RIWERM. We used the linear-in-parameter models (10) with the Gaussian kernels (introduced in Section 3.2.2) as basis functions for learning the input-output relation and the importance (or the relative importance) in all the experiments:

$$\phi_i(\mathbf{x}) = \exp \left\{ -\frac{\|\mathbf{x} - \mathbf{c}_i^f\|^2}{2\sigma_f^2} \right\} \quad \text{and} \quad \psi_i(\mathbf{x}) = \exp \left\{ -\frac{\|\mathbf{x} - \mathbf{c}_i^g\|^2}{2\sigma_g^2} \right\},$$

where σ_f and σ_g are the bandwidths of the Gaussian kernels, and \mathbf{c}_i^f and \mathbf{c}_i^g are the kernel centers randomly chosen from $\{\mathbf{x}_j^{\text{te}}\}_{j=1}^{n_{\text{te}}}$ [24, 26]. We set $b_f = b_g = 50$ in all the experiments.

As suggested in Section 5.1, we used the squared loss in the one-step approach for computational efficiency. We also employed the IRLS algorithm for optimizing Tukey’s bisquare loss in the one-step approach. For better comparison, we reported the results of the baseline methods using both the squared loss and Tukey’s bisquare loss.

The experimental results of the toy regression problem are summarized in Table 1. Note that when the target function f^* is perfectly learned, the mean squared error is the variance of noise ϵ , i.e., 0.01. Therefore, our method significantly mitigates the influence of covariate shift. Since the IRLS algorithm is needed when using Tukey’s bisquare loss, the training should take longer time than that when using the squared loss, and we confirmed this fact from the results in Table 1.

5.3.2 Experiments on Regression and Binary Classification Benchmark Datasets

Below, we report the results of experiments on regression benchmark datasets from UCI² and binary classification benchmark datasets from LIBSVM³.

²<https://archive.ics.uci.edu/ml/datasets.php>

³<https://www.csie.ntu.edu.tw/~cjlin/libsvmtools/datasets/>

Table 2: Mean squared test errors/mean test misclassification rates averaged over 100 trials on regression/binary classification benchmark datasets. The numbers in the brackets are the standard deviations. All the error values are normalized so that the mean error by “ERM” will be one. For each dataset, the best method and comparable ones based on the *paired t-test* at the significance level 5% are described in bold face. The upper half are regression datasets and the lower half are binary classification datasets.

Dataset	ERM	EIWERM	RIWERM	one-step
auto	1.00 (0.22)	1.08 (0.25)	1.08 (0.23)	0.99 (0.21)
bike	1.00 (0.10)	0.97 (0.10)	0.98 (0.10)	0.95 (0.08)
parkinsons	1.00 (0.28)	0.93 (0.17)	0.92 (0.16)	0.76 (0.05)
wine	1.00 (0.22)	0.95 (0.12)	0.95 (0.14)	0.90 (0.07)
australian	31.62 (17.88)	30.70 (16.35)	29.82 (14.83)	25.57 (12.74)
breast	22.13 (10.36)	21.82 (11.20)	22.00 (13.38)	16.55 (9.09)
diabetes	43.35 (9.56)	41.67 (8.66)	43.26 (8.42)	38.57 (6.36)
heart	34.91 (12.45)	32.06 (11.05)	33.39 (12.24)	31.39 (10.36)
sonar	39.03 (6.69)	38.77 (6.37)	38.83 (7.15)	37.69 (7.17)

We considered experimental settings with both synthetically created covariate shift and naturally occurring covariate shift. To perform train-test split for the datasets with naturally occurring covariate shift, we followed [55], [56], and [57] to separate the auto mpg dataset, the bike sharing dataset, the parkinsons dataset, and the wine quality dataset based on different origins, different semesters, different age ranges, and different types, respectively. In the rest of the datasets, we synthetically introduced covariate shift in the following way similarly to [58]. First, we used Z-score normalization to preprocess all the input samples. Then, an example (\mathbf{x}, y) was assigned to the training dataset with probability $\exp(v)/(1 + \exp(v))$ and to the test dataset with probability $1/(1 + \exp(v))$, where $v = 16\mathbf{w}^\top \mathbf{x}/\sigma$, σ is the standard deviation of $\mathbf{w}^\top \mathbf{x}$, and $\mathbf{w} \in \mathbb{R}^d$ is some given projection vector. To ensure that the methods are tested in challenging covariate shift situations, we randomly sampled projection directions and chose the one such that the classifier trained on the training dataset generalizes worst to the test dataset for train-test split.

By following the above procedure, we split the datasets into training datasets and test datasets (with some randomness in synthetic cases). Then we sampled a certain number (depending on the size of the dataset) of training samples and test input samples for training. We used the rest of test samples for evaluating the performance. We ran 100 trials for each dataset.⁴ As discussed in Section 5.1, we used the squared loss as the surrogate loss function for all the methods including the one-step approach in the experiments.

The experimental results on benchmark datasets are summarized in Table 2. The table shows the proposed one-step approach outperforms or is comparable to the baseline methods with the best performance, which suggests that it is a promising method for covariate shift

⁴It means that we conduct the experiment for each dataset 100 times with different random draws of training and test samples.

Table 3: Mean test classification accuracy averaged over 5 trials on image datasets with neural networks. The numbers in the brackets are the standard deviations. For each dataset, the best method and comparable ones based on the *paired t-test* at the significance level 5% are described in bold face.

Dataset	Shift Level (a, b)	ERM	EIWERM	RIWERM	one-step
Fashion-MNIST	(2, 4)	81.71(0.17)	84.02(0.18)	84.12(0.06)	85.07(0.08)
	(2, 5)	72.52(0.54)	76.68(0.27)	77.43(0.29)	78.83(0.20)
	(2, 6)	60.10(0.34)	65.73(0.34)	66.73(0.55)	69.23(0.25)
Kuzushiji-MNIST	(2, 4)	77.09(0.18)	80.92(0.32)	81.17(0.24)	82.45(0.12)
	(2, 5)	65.06(0.26)	71.02(0.50)	72.16(0.19)	74.03(0.16)
	(2, 6)	51.24(0.30)	58.78(0.38)	60.14(0.93)	62.70(0.55)

adaptation.

5.3.3 Multi-class Classification Experiments with Neural Networks

Finally, we designed a covariate shift setting and conducted experiments on the Fashion-MNIST [59] and Kuzushiji-MNIST [60] benchmark datasets for image classification using convolutional neural networks (CNNs).

Based on the fact that the labels of the images from those datasets are invariant to rotation transformation, we introduced covariate shift to the image datasets in the following way: we rotated each image I_i in the training sets by angle θ_i , where $\theta_i/180^\circ$ was drawn from a beta distribution $\text{Beta}(a, b)$, and rotated each image J_i in the test sets by angle ϕ_i , where $\phi_i/180^\circ$ was drawn from another beta distribution $\text{Beta}(b, a)$. The parameters a and b control the shift level, and we tested three different levels in our experiments: $(a, b) = (2, 4)$, $(2, 5)$, and $(2, 6)$. Since our experiments were conducted in an inductive manner, we also rotated each image I_i in the training sets by angle ψ_i , where $\psi_i/180^\circ$ was drawn from the beta distribution $\text{Beta}(b, a)$ to obtain the unlabeled test images for training.

We used Algorithm 2 as our implementation of the one-step approach. We used the softmax cross-entropy loss as a surrogate loss and use 5-layer CNNs, which consist of 2 convolutional layers with pooling and 3 fully connected layers, to model the classifier f and the weight model g . In order to learn useful weights, we pretrained g in a binary classification problem whose goal is to discriminate between $\{\mathbf{x}_i^{\text{tr}}\}_{i=1}^{n_{\text{tr}}}$ and $\{\mathbf{x}_j^{\text{te}}\}_{j=1}^{n_{\text{te}}}$ and froze the parameters in the first two convolutional layers. We trained f and g for 20 rounds for the one-step approach, where a round consists of 5 epochs of training g followed by 10 epochs of training f : we trained the models for 300 epochs in total. Details can be found in [31].

The experimental results summarized in Table 3 verify the effectiveness of our one-step approach in image classification problems with neural networks. Specifically, the table shows that the ordinary ERM performs poorly under covariate shift, the weighted methods all improve the performance, and the one-step approach further improves the performance especially under large covariate shift (i.e., the difference between shift parameters a and b is large).

6 Dynamic Importance Weighting

So far, we have discussed covariate shift as the primal target for transfer learning. In this section, we consider the *full-distribution shift* problem and introduce a novel method, dynamic importance weighting (DIW) [46], for making importance weighting work well for deep learning under distribution shift.

6.1 Motivation and Problem Setup

Let us consider the problem setup of *full-distribution shift*, where the training data $\{(\mathbf{x}_i^{\text{tr}}, y_i^{\text{tr}})\}_{i=1}^{n_{\text{tr}}}$ are drawn from $p_{\text{tr}}(\mathbf{x}, y)$, the test data $\{(\mathbf{x}_j^{\text{te}}, y_j^{\text{te}})\}_{j=1}^{n_{\text{te}}}$ are drawn from $p_{\text{te}}(\mathbf{x}, y)$, and $p_{\text{tr}}(\mathbf{x}, y) \neq p_{\text{te}}(\mathbf{x}, y)$. Then, importance weighting (IW) under *full-distribution shift* can be formulated as

$$\mathbb{E}_{(\mathbf{x}^{\text{te}}, y^{\text{te}}) \sim p_{\text{te}}(\mathbf{x}, y)} [\ell(f(\mathbf{x}^{\text{te}}), y^{\text{te}})] = \mathbb{E}_{(\mathbf{x}^{\text{tr}}, y^{\text{tr}}) \sim p_{\text{tr}}(\mathbf{x}, y)} [w(\mathbf{x}^{\text{tr}}, y^{\text{tr}}) \ell(f(\mathbf{x}^{\text{tr}}), y^{\text{tr}})], \quad (12)$$

where the *importance* is $w(\mathbf{x}, y) = p_{\text{te}}(\mathbf{x}, y) / p_{\text{tr}}(\mathbf{x}, y)$. Here we assume that we have a tiny set of validation data from $p_{\text{te}}(\mathbf{x}, y)$. For brevity, we abbreviate *importance estimation* in Section 3.1 as *weight estimation* (WE) and abbreviate *importance-weighted ERM* as *weighted classification* (WC).

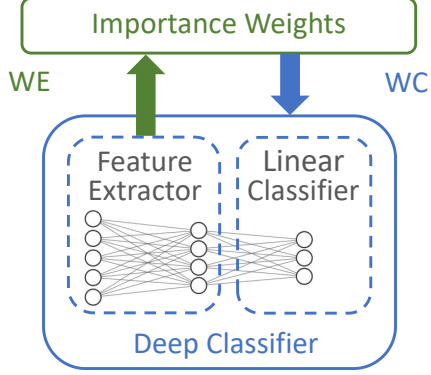
IW works very well if the form of data is simple (e.g., some linear model suffices), and it has been the common practice of non-deep learning under distribution shift [28]. However, IW cannot work well if the form of data is complex [61]. Recall that for the k -class classification problem with input domain $\mathcal{X} \subset \mathbb{R}^{d_{\text{in}}}$ and output domain $\mathcal{Y} := [k]$, $w(\mathbf{x}, y)$ processes $(d_{\text{in}} + 1)$ -dimensional or $(d_{\text{in}} + k)$ -dimensional input depending on how y is encoded and $f(\mathbf{x})$ processes d_{in} -dimensional input, and consequently WE is not necessarily easier than WC. Hence, when a deep model is used in WC, more *expressive power* may be needed in WE.

Here we improve IW for deep learning under distribution shift. Nevertheless, WE and WC are different tasks with different goals, and it is difficult to boost the expressive power of WE for three reasons:

- some WE methods are *model-free* (e.g., *KMM* in Section 3.2.1), i.e., they assign weights to data without a model of w ;
- other WE methods are *model-based* and also *model-independent* (e.g., *LSIF* and *uLSIF* in Section 3.2.2), but the optimizations are constrained due to $\mathbb{E}_{p_{\text{tr}}(\mathbf{x}, y)} [w(\mathbf{x}, y)] = \mathbb{E}_{p_{\text{te}}(\mathbf{x}, y)} [1] = 1$ and incompatible with stochastic solvers;
- most powerful deep models nowadays are hard to train with the WE optimizations since they are *designed for classification*, even if we ignore the constraint or satisfy it within each mini-batch.

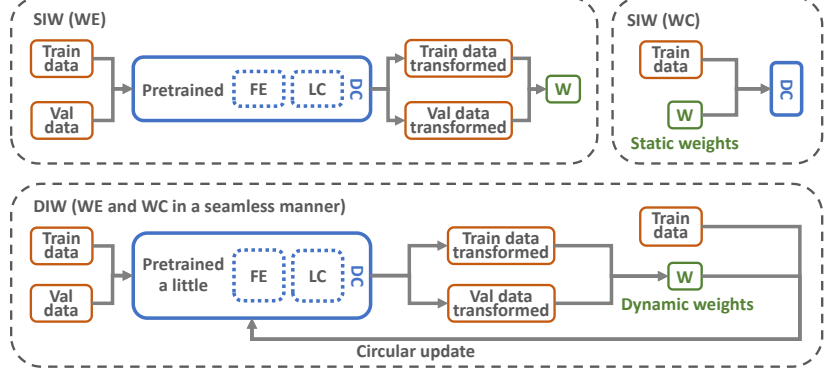
Therefore, it sounds better to boost the expressive power by an external *feature extractor* (FE). For instance, we may rely on f that is a deep model chosen for the classification problem to be solved. Going along this way, we encounter the *circular dependency* in Figure 3: originally we need w to train f ; now we need a trained f to estimate w . It becomes a chicken-or-egg causality dilemma.

We think of two possible ways to solve the circular dependency, one *pipelined* and one *end-to-end*. The pipelined solution pretrains a deep classifier (DC) from unweighted training



Blue arrow depicts WC depending on WE; green arrow depicts WE depending on WC—this makes a circle.

Figure 3: Circular dependency.



SIW/DIW stands for static/dynamic importance weighting; FE is short for feature extractor, and LC/DC is for linear/deep classifier; W is a set of weights. Circular update is employed to solve circular dependency.

Figure 4: Illustrations of SIW and DIW.

data, and creates an FE from this DC; then, WE is carried out on the data transformed by the FE. Since the weights cannot change, we call this method *static importance weighting* (SIW), as illustrated in the top diagram of Figure 4. Here, the DC is biased to the training data, and so is the FE, which could be empirically confirmed [46]. As a result, this naive pipelined solution is only slightly better than no FE unfortunately.

To overcome the bias of SIW, we propose *dynamic importance weighting* (DIW) [46] as an end-to-end solution; see the bottom diagram of Figure 4. DIW iterates between WE (on the transformed data) and WC (for updating the DC and FE) and combines them in a seamless manner. This end-to-end solution can gradually *improve the importance weight and reduce the bias of f* .

6.2 Dynamic Importance Weighting

Here we introduce the details of the proposed method, dynamic importance weighting (DIW), including the weighted classification, non-linear transformation of data, practical choices of the transformation, and the distribution matching in DIW.

6.2.1 Weighted Classification

In this section, we assume that our classifier to be trained is a deep network parameterized by θ , denoted by $f_\theta : \mathcal{X} \rightarrow \mathbb{R}^k$. Let $\ell : \mathbb{R}^k \times \mathcal{Y} \rightarrow \mathbb{R}_+$ be a *surrogate loss function* for k -class classification, e.g., the *softmax cross-entropy loss*. The classification risk of f_θ is defined as

$$R(f_\theta) = \mathbb{E}_{p_{te}(\mathbf{x}, y)} [\ell(f_\theta(\mathbf{x}), y)], \quad (13)$$

which is the performance measure we would like to optimize. According to Eq. (12), if $w(\mathbf{x}, y)$ is given or $\mathcal{W} = \{w_i = w(\mathbf{x}_i^{\text{tr}}, y_i^{\text{tr}})\}_{i=1}^{n_{\text{tr}}}$ is given, $R(f_\theta)$ can be approximated by

$$\hat{R}(f_\theta) = \frac{1}{n_{\text{tr}}} \sum_{i=1}^{n_{\text{tr}}} w_i \ell(f_\theta(\mathbf{x}_i^{\text{tr}}), y_i^{\text{tr}}), \quad (14)$$

which is the objective of WC. With the *optimal weights*, the weighted empirical risk in Eq. (14) is an *unbiased estimator* of the risk in Eq. (13), and hence the trained classifier as the minimizer of $\widehat{R}(\mathbf{f}_\theta)$ should converge to the minimizer of $R(\mathbf{f}_\theta)$ as n_{tr} approaches infinity [20, 22, 23, 24, 25, 26].

6.2.2 Non-linear Transformation of Data

Now, the issue is how to estimate the function w or the set \mathcal{W} . As discussed earlier in Section 6.1, we should boost the expressive power externally but not internally. This means we should apply a *non-linear transformation* of data rather than directly modeling $w(\mathbf{x}, y)$ or $p_{\text{tr}}(\mathbf{x}, y)$ and $p_{\text{te}}(\mathbf{x}, y)$ by deep networks. Let $\pi : \mathcal{X} \times \mathcal{Y} \rightarrow \mathbb{R}^{d_r}$ or $\pi : \mathcal{X} \times \mathcal{Y} \rightarrow \mathbb{R}^{d_r-1} \times \mathcal{Y}$ be a transformation, where d_r is the reduced dimension and $d_r \ll d$; let $\mathbf{z} = \pi(\mathbf{x}, y)$ be the transformed random variable, whose source of randomness is (\mathbf{x}, y) exclusively. By applying π , we expect that WE on \mathbf{z} will be much easier than WE on (\mathbf{x}, y) . The feasibility of applying π is justified below.

Theorem 5. [46] *For a fixed, deterministic and invertible transformation $\pi : (\mathbf{x}, y) \mapsto \mathbf{z}$, let $p_{\text{tr}}(\mathbf{z})$ and $p_{\text{te}}(\mathbf{z})$ be the probability density functions induced by $p_{\text{tr}}(\mathbf{x}, y)$, $p_{\text{te}}(\mathbf{x}, y)$, and π . Then,*

$$w(\mathbf{x}, y) = \frac{p_{\text{te}}(\mathbf{x}, y)}{p_{\text{tr}}(\mathbf{x}, y)} = \frac{p_{\text{te}}(\mathbf{z})}{p_{\text{tr}}(\mathbf{z})} = w(\mathbf{z}). \quad (15)$$

Proof. Let $F_{\text{tr}}(\mathbf{x}, y)$, $F_{\text{te}}(\mathbf{x}, y)$, $F_{\text{tr}}(\mathbf{z})$ as well as $F_{\text{te}}(\mathbf{z})$ be the corresponding cumulative distribution functions. Then the fundamental theorem of calculus, and three properties of π namely π is fixed, deterministic, and invertible, it holds that

$$p_{\text{tr}}(\mathbf{x}, y) d\mathbf{x} = dF_{\text{tr}}(\mathbf{x}, y) = dF_{\text{tr}}(\mathbf{z}) = p_{\text{tr}}(\mathbf{z}) d\mathbf{z}, \quad (16)$$

$$p_{\text{te}}(\mathbf{x}, y) d\mathbf{x} = dF_{\text{te}}(\mathbf{x}, y) = dF_{\text{te}}(\mathbf{z}) = p_{\text{te}}(\mathbf{z}) d\mathbf{z}, \quad (17)$$

where d denotes the differential operator, and

$$dF_*(\mathbf{x}, y) = \frac{\partial}{\partial \mathbf{x}} \left(\sum_{y' \leq y} \int_{\mathbf{x}' \leq \mathbf{x}} p_*(\mathbf{x}', y') d\mathbf{x}' - \sum_{y' < y} \int_{\mathbf{x}' \leq \mathbf{x}} p_*(\mathbf{x}', y') d\mathbf{x}' \right) \cdot d\mathbf{x},$$

where $*$ indicates tr or te. For simplicity, the continuous random variable \mathbf{x} and the discrete random variable y are considered separately. Dividing Eq. (17) by Eq. (16) proves Eq. (15). \square

Theorem 5 requires that π satisfies three properties: we cannot guarantee $dF_{\text{tr}}(\mathbf{z}) = p_{\text{tr}}(\mathbf{z}) d\mathbf{z}$ if π is not fixed or $dF_{\text{tr}}(\mathbf{x}, y) = dF_{\text{tr}}(\mathbf{z})$ if π is neither deterministic nor invertible. As a result, when \mathcal{W} is computed in WE, \mathbf{f}_θ is regarded as fixed, and it could be switched to the *evaluation mode* from the *training mode* to avoid the randomness due to dropout [62] or similar randomized algorithms. The invertibility of π is non-trivial: it assumes that $\mathcal{X} \times \mathcal{Y}$ is generated by a manifold $\mathcal{M} \subset \mathbb{R}^{d_m}$ with an intrinsic dimension $d_m \leq d_r$, and π^{-1} recovers the generating function from \mathcal{M} to $\mathcal{X} \times \mathcal{Y}$. If π is from parts of \mathbf{f}_θ , \mathbf{f}_θ must be a reasonably good classifier so that π compresses $\mathcal{X} \times \mathcal{Y}$ back to \mathcal{M} . This finding is the circular dependency in Figure 3, which is the major theoretical contribution.

6.2.3 Practical Choices of π

It seems obvious that π can be f_θ as a whole or without its topmost layer. However, the latter drops y and corresponds to assuming

$$p_{\text{tr}}(y | \mathbf{x}) = p_{\text{te}}(y | \mathbf{x}) \implies \frac{p_{\text{te}}(\mathbf{x}, y)}{p_{\text{tr}}(\mathbf{x}, y)} = \frac{p_{\text{te}}(\mathbf{x}) \cdot p_{\text{te}}(y | \mathbf{x})}{p_{\text{tr}}(\mathbf{x}) \cdot p_{\text{tr}}(y | \mathbf{x})} = \frac{p_{\text{te}}(\mathbf{x})}{p_{\text{tr}}(\mathbf{x})} = \frac{p_{\text{te}}(\mathbf{z})}{p_{\text{tr}}(\mathbf{z})}, \quad (18)$$

which is only possible under *covariate shift* [34, 20, 24, 25]. It is conceptually a bad idea to attach y to the latent representation of \mathbf{x} , since the distance metric on \mathcal{Y} is completely different. A better idea to take the information of y into account may consist of three steps. First, estimate $p_{\text{te}}(y)/p_{\text{tr}}(y)$; second, partition $\{(\mathbf{x}_i^{\text{tr}}, y_i^{\text{tr}})\}_{i=1}^{n_{\text{tr}}}$ and $\{(\mathbf{x}_j^{\text{te}}, y_j^{\text{te}})\}_{j=1}^{n_{\text{te}}}$ according to y ; third, invoke WE k times on k partitions separately based on the following identity: let $w_y = p_{\text{te}}(y)/p_{\text{tr}}(y)$, then

$$\frac{p_{\text{te}}(\mathbf{x}, y)}{p_{\text{tr}}(\mathbf{x}, y)} = \frac{p_{\text{te}}(y) \cdot p_{\text{te}}(\mathbf{x} | y)}{p_{\text{tr}}(y) \cdot p_{\text{tr}}(\mathbf{x} | y)} = w_y \cdot \frac{p_{\text{te}}(\mathbf{x} | y)}{p_{\text{tr}}(\mathbf{x} | y)} = w_y \cdot \frac{p_{\text{te}}(\mathbf{z} | y)}{p_{\text{tr}}(\mathbf{z} | y)}. \quad (19)$$

That being said, in a small mini-batch, invoking WE k times on even smaller partitions might be remarkably less reliable than invoking it once on the whole mini-batch.

To this end, we propose an alternative choice $\pi : (\mathbf{x}, y) \mapsto \ell(f_\theta(\mathbf{x}), y)$ that is motivated as follows. In practice, we are not sure about the existence of \mathcal{M} , we cannot check whether $d_{\text{m}} \leq d_{\text{r}}$ when \mathcal{M} indeed exists, or it is computationally hard to confirm that π is invertible. Consequently, Eqs. (18) and (19) may not hold or only hold approximately. As a matter of fact, Eq. (12) also only holds approximately after replacing the expectations with empirical averages, and then it may be too much to stick to the optimal solution $w(\mathbf{x}, y)$. According to Eq. (12), there exists $w(\mathbf{x}, y)$ such that for all possible $h : \mathcal{X} \times \mathcal{Y} \rightarrow \mathbb{R}$,

$$\begin{aligned} \frac{1}{n_{\text{te}}} \sum_{j=1}^{n_{\text{te}}} h(\mathbf{x}_j^{\text{te}}, y_j^{\text{te}}) &\approx \mathbb{E}_{p_{\text{te}}(\mathbf{x}, y)}[h(\mathbf{x}, y)] \\ &\approx \mathbb{E}_{p_{\text{tr}}(\mathbf{x}, y)}[w(\mathbf{x}, y)h(\mathbf{x}, y)] \approx \frac{1}{n_{\text{tr}}} \sum_{i=1}^{n_{\text{tr}}} \hat{w}_i h(\mathbf{x}_i^{\text{tr}}, y_i^{\text{tr}}), \end{aligned}$$

where \hat{w}_i is an estimated importance weight for $i = 1, \dots, n_{\text{tr}}$. This goal, *IW for everything*, is too general and its only solution is $\hat{w}_i = w(\mathbf{x}_i^{\text{tr}}, y_i^{\text{tr}})$; nonetheless, it is more than needed—*IW for classification* is our current goal.

Specifically, the goal of DIW is to find a set of weights $\hat{\mathcal{W}} = \{\hat{w}_i\}_{i=1}^{n_{\text{tr}}}$ such that for $\ell(f_\theta(\mathbf{x}), y)$,

$$\frac{1}{n_{\text{te}}} \sum_{j=1}^{n_{\text{te}}} \ell(f_\theta(\mathbf{x}_j^{\text{te}}, y_j^{\text{te}})) \Big|_{\theta=\theta_t} \approx \frac{1}{n_{\text{tr}}} \sum_{i=1}^{n_{\text{tr}}} \hat{w}_i \ell(f_\theta(\mathbf{x}_i^{\text{tr}}, y_i^{\text{tr}})) \Big|_{\theta=\theta_t}, \quad (20)$$

where the left- and right-hand sides are conditioned on $\theta = \theta_t$, and θ_t holds model parameters at a certain time point t of training. After $\hat{\mathcal{W}}$ is found, θ_t will be updated to θ_{t+1} , and the current f_θ will move to the next f_θ ; then, we need to find a new set of weights satisfying Eq. (20) again. Compared with the general goal of IW, the goal of DIW is special and easy to achieve, and then there may be many different solutions, any of which can be used to replace $\mathcal{W} = \{w_i\}_{i=1}^{n_{\text{tr}}}$ in $\hat{R}(f_\theta)$. The above argument elaborates the motivation of $\pi : (\mathbf{x}, y) \mapsto \ell(f_\theta(\mathbf{x}), y)$. This is possible thanks to the *dynamic nature of weights* in DIW, which is the major methodological contribution.

Algorithm 3 Dynamic importance weighting (in a mini-batch).

Require: a training mini-batch \mathcal{S}^{tr} , a teidation mini-batch \mathcal{S}^{te} , the current model f_{θ_t}

Hidden-layer-output transformation version:

Loss-value transformation version:

- | | |
|---|---|
| <ol style="list-style-type: none"> 1: forward the input parts of \mathcal{S}^{tr} & \mathcal{S}^{te} 2: retrieve the hidden-layer outputs \mathcal{Z}^{tr} & \mathcal{Z}^{te} 3: partition \mathcal{Z}^{tr} & \mathcal{Z}^{te} into $\{\mathcal{Z}_y^{\text{tr}}\}_{y=1}^k$ & $\{\mathcal{Z}_y^{\text{te}}\}_{y=1}^k$ 4: for $y = 1, \dots, k$ do 5: match $\mathcal{Z}_y^{\text{tr}}$ & $\mathcal{Z}_y^{\text{te}}$ to obtain $\hat{\mathcal{W}}_y$ 6: multiply all $w_i \in \hat{\mathcal{W}}_y$ by w_y 7: end for 8: compute the loss values of \mathcal{S}^{tr} as \mathcal{L}^{tr} 9: weight the empirical risk $\hat{R}(f_{\theta})$ by $\{\hat{\mathcal{W}}_y\}_{y=1}^k$ 10: backward $\hat{R}(f_{\theta})$ and update θ | <ol style="list-style-type: none"> 1: forward the input parts of \mathcal{S}^{tr} & \mathcal{S}^{te} 2: compute the loss values as \mathcal{L}^{tr} & \mathcal{L}^{te} 3: match \mathcal{L}^{tr} & \mathcal{L}^{te} to obtain $\hat{\mathcal{W}}$ 4: weight the empirical risk $\hat{R}(f_{\theta})$ by $\hat{\mathcal{W}}$ 5: backward $\hat{R}(f_{\theta})$ and update θ |
|---|---|
-

6.2.4 Distribution Matching

Finally, we perform distribution matching between the set of transformed training data $\{z_i^{\text{tr}}\}_{i=1}^{n_{\text{tr}}}$ and the set of transformed validation data $\{z_j^{\text{te}}\}_{j=1}^{n_{\text{te}}}$. Let \mathcal{H} be a Hilbert space of real-valued functions on $\mathbb{R}^{d_{\text{tr}}}$ with an inner product $\langle \cdot, \cdot \rangle_{\mathcal{H}}$, or \mathcal{H} be a *reproducing kernel Hilbert space*, where $k : (z, z') \mapsto \langle \phi_k(z), \phi_k(z') \rangle_{\mathcal{H}}$ is the reproducing kernel of \mathcal{H} and $\phi_k : \mathbb{R}^{d_{\text{tr}}} \rightarrow \mathcal{H}$ is the kernel-induced feature map [5]. Then, we perform *kernel mean matching* [23] in Section 3.2.1 as follows.

Let $\mu_{\text{tr}} = \mathbb{E}_{w(z) \cdot p_{\text{tr}}(x, y)}[\phi_k(z)]$ and $\mu_{\text{te}} = \mathbb{E}_{p_{\text{te}}(x, y)}[\phi_k(z)]$ be the kernel embeddings of $p_{\text{tr}} \cdot w$ and p_{te} in \mathcal{H} , the discrepancy between the two can be approximated by

$$\begin{aligned} \|\mu_{\text{tr}} - \mu_{\text{te}}\|_{\mathcal{H}}^2 &\approx \left\| \frac{1}{n_{\text{tr}}} \sum_{i=1}^{n_{\text{tr}}} w_i \phi_k(z_i^{\text{tr}}) - \frac{1}{n_{\text{te}}} \sum_{j=1}^{n_{\text{te}}} \phi_k(z_j^{\text{te}}) \right\|_{\mathcal{H}}^2 \\ &\propto \mathbf{w}^{\top} \mathbf{K} \mathbf{w} - 2 \mathbf{k}^{\top} \mathbf{w} + \text{Const.}, \end{aligned} \quad (21)$$

where $\mathbf{w} \in \mathbb{R}^{n_{\text{tr}}}$ is the weight vector, $\mathbf{K} \in \mathbb{R}^{n_{\text{tr}} \times n_{\text{tr}}}$ is a kernel matrix such that $K_{ij} = k(z_i^{\text{tr}}, z_j^{\text{tr}})$, and $\mathbf{k} \in \mathbb{R}^{n_{\text{tr}}}$ is a vector such that $k_i = \frac{n_{\text{tr}}}{n_{\text{te}}} \sum_{j=1}^{n_{\text{te}}} k(z_i^{\text{tr}}, z_j^{\text{te}})$. In practice, Eq. (21) is minimized subject to $0 \leq w_i \leq B$ and $|\frac{1}{n_{\text{tr}}} \sum_{i=1}^{n_{\text{tr}}} w_i - 1| \leq \epsilon$ where $B > 0$ and $\epsilon > 0$ are hyperparameters as the upper bound of weights and the slack variable of $\frac{1}{n_{\text{tr}}} \sum_{i=1}^{n_{\text{tr}}} w_i = 1$. Eq. (21) is the objective of WE. The whole DIW is shown in Algorithm 3, which is our major algorithmic contribution.

6.3 Experiments

In this section, we verify the effectiveness of DIW.⁵ We first compare DIW based on loss-value transformation with baseline methods under label noise and class-prior shift. We then report the results of ablation studies.

⁵Our implementation of DIW is available at <https://github.com/TongtongFANG/DIW>.

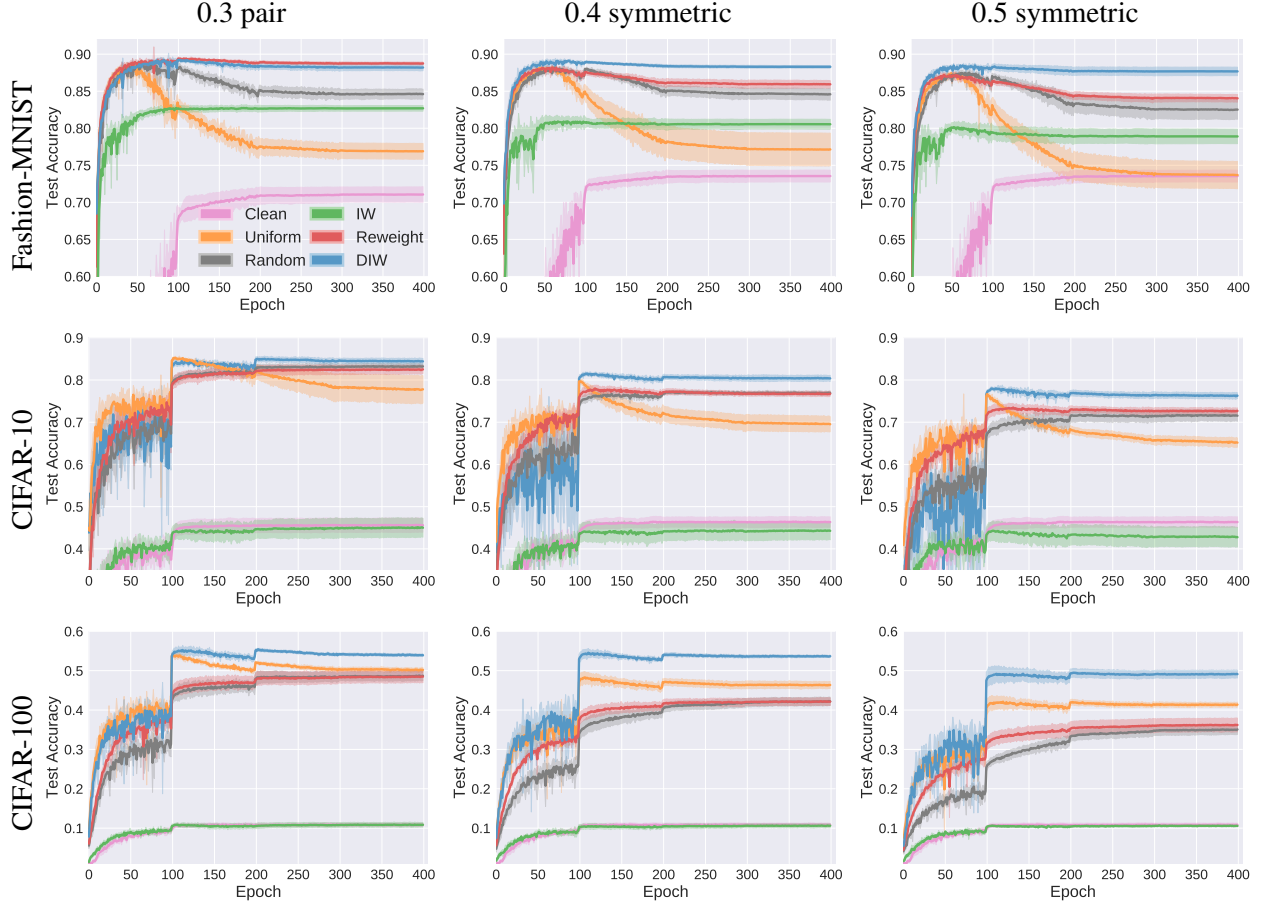


Figure 5: Experimental results on Fashion-MNIST and CIFAR-10/100 under label noise (5 trials).

6.3.1 Baselines

There are five baseline methods involved in our experiments:

- *Clean* discards the training data and uses the validation data for training;
- *Uniform* does not weight the training data, i.e., the weights are all ones;
- *Random* draws random weights following the *rectified Gaussian distribution*;
- *IW* is kernel mean matching without any non-linear transformation [23];
- *Reweight* is learning to reweight [63].

All baselines were implemented with PyTorch.⁶ Note that in each mini-batch, DIW computes \mathcal{W} and then updates \mathbf{f}_θ , while Reweight updates \mathbf{f}_θ and then updates \mathcal{W} . Moreover, Reweight updates \mathcal{W} in epoch one, while DIW pretrains \mathbf{f}_θ in epoch one to equally go over all the training data once.

⁶We implemented Reweight to ensure same random samplings of data and initialization of models.

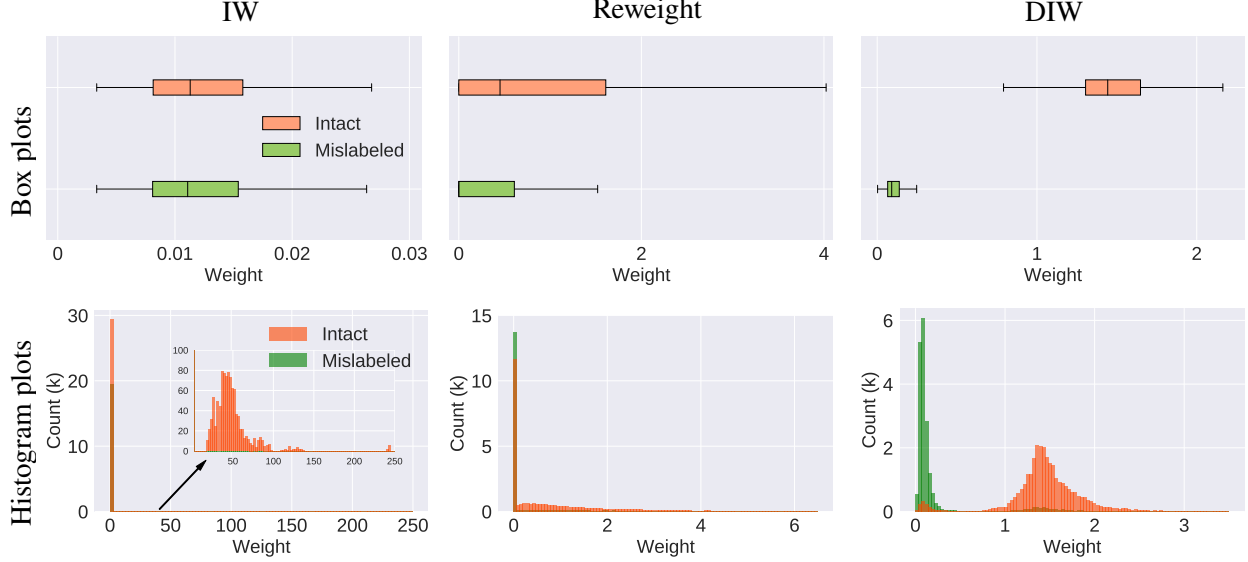


Figure 6: Statistics of weight distributions on CIFAR-10 under 0.4 symmetric flip.

6.3.2 Setup

The experiments were based on three widely used benchmark datasets *Fashion-MNIST* [59], *CIFAR-10*, and *CIFAR-100* [64]. For the set of validation data,

- 1,000 random clean data in total were used in the label-noise experiments;
- 10 random data per class were used in the class-prior-shift experiments.

The validation data were included in the training data, as required by Reweight. Then,

- for Fashion-MNIST, LeNet-5 [65] was trained by SGD [50];
- for CIFAR-10/100, ResNet-32 [66] was trained by Adam [67].

For fair comparisons, we normalized \mathcal{W} to make the average weight 1 in each mini-batch. For clear comparisons, there was no data augmentation. More details can be found in [46].

6.3.3 Label-noise Experiments

Two major class-conditional noise models were considered:

- *pair flip* [68], where a label j , if it gets mislabeled, must flip to class $(j \bmod k + 1)$;
- *symmetric flip* [69], where a label may flip to all other classes with equal probability.

We set the noise rate as 0.3 for pair flip and 0.4 or 0.5 for symmetric flip. The experimental results are reported in Figure 5. We can see that DIW outperforms the baselines. As the noise rate increases, DIW stays reasonably robust and the baselines tend to overfit the noisy labels.

To better understand how DIW contributes to learning robust models, we take a look at the learned weights in the final epoch. As shown in Figure 6, DIW can successfully identify intact/mislabeled training data and automatically up-/down-weight them, while others cannot effectively identify them. This confirms that DIW can improve the weights and thus reduce the bias of the model.

Table 4: Mean accuracy (standard deviation) in percentage on Fashion-MNIST under class-prior shift (5 trials). Best and comparable methods (paired t -test at significance level 5%) are highlighted in bold.

	$\rho = 100$	$\rho = 200$
Clean	63.38 (2.59)	63.38 (2.59)
Uniform	83.48 (1.26)	79.12 (1.18)
Random	83.11 (1.70)	79.38 (0.96)
IW	83.45 (1.10)	80.25 (2.23)
Reweight	81.96 (1.74)	79.37 (2.38)
DIW	84.02 (1.82)	81.37 (0.95)
Truth	83.29 (1.11)	80.22 (2.13)

Table 5: Mean distance (standard deviation) from the learned weights to the true weights on Fashion-MNIST under class-prior shift (5 trials). Best and comparable methods (paired t -test at significance level 5%) are highlighted in bold.

	$\rho = 100$	MAE	RMSE
IW		1.10 (0.03)	10.19 (0.33)
Reweight		1.66 (0.02)	5.65 (0.20)
DIW		0.45 (0.02)	3.19 (0.07)
	$\rho = 200$	MAE	RMSE
IW		1.03 (0.04)	9.99 (0.38)
Reweight		1.64 (0.05)	6.07 (0.86)
DIW		0.46 (0.06)	3.67 (0.13)

6.3.4 Class-prior-shift Experiments

We imposed class-prior shift on Fashion-MNIST following [41]:

- the classes were divided into majority classes and minority classes, where the fraction of the minority classes is $\mu < 1$;
- the training data were drawn from every majority class using a sample size, and from every minority class using another sample size, where the ratio of these two sample sizes was $\rho > 1$;
- the test data were evenly sampled from all classes.

We fixed $\mu = 0.2$ and tried $\rho = 100$ and $\rho = 200$. A new baseline *Truth* was added for reference, where the true weights were used, i.e., $1 - \mu + \mu/\rho$ and $\mu + \rho - \mu\rho$ for the majority/minority classes.

The experimental results are reported in Table 4, where we can see that DIW again outperforms the baselines. Table 5 contains the *mean absolute error* (MAE) and *root mean square error* (RMSE) from the weights learned by IW, Reweight, and DIW to the true weights, as the unit test under class-prior shift. The results confirm that the weights learned by DIW are closer to the true weights.

6.3.5 Ablation Study

As shown in Figure 4, DIW comprises many options, which means that DIW can have a complicated algorithm design. Starting from IW,

- introducing feature extractor (FE) yields SIW;
- based on SIW, updating \mathcal{W} yields DIW1;
- based on DIW1, updating FE yields DIW2;
- based on DIW2, pretraining FE yields DIW3.

Table 6: Mean accuracy (standard deviation) in percentage on Fashion-MNIST (F-MNIST for short) and CIFAR-10/100 under label noise (5 trials). Best and comparable methods (paired t -test at significance level 5%) are highlighted in bold. p/s is short for pair/symmetric flip.

	Noise	IW	SIW-F	SIW-L	DIW1-F	DIW2-F	DIW3-F	DIW1-L	DIW2-L	DIW3-L
F-MNIST	0.3 p	82.69	82.41	85.46	87.60	87.67	87.54	87.04	88.19	86.68
		(0.38)	(0.46)	(0.29)	(0.07)	(0.37)	(0.25)	(0.51)	(0.43)	(1.42)
	0.4 s	80.54	82.36	88.68	87.45	87.04	88.29	88.98	88.29	87.89
		(0.66)	(0.65)	(0.23)	(0.22)	(0.30)	(0.16)	(0.19)	(0.18)	(0.43)
	0.5 s	78.90	81.29	87.49	87.27	86.41	87.28	87.70	87.67	86.74
		(0.97)	(0.68)	(0.23)	(0.38)	(0.36)	(0.18)	(0.15)	(0.57)	(1.19)
CIFAR-10	0.3 p	45.02	74.61	80.45	82.75	81.19	81.76	81.73	84.44	83.80
		(2.25)	(0.51)	(0.89)	(0.57)	(0.81)	(0.70)	(0.54)	(0.70)	(0.93)
	0.4 s	44.31	65.58	76.39	78.23	77.48	78.75	75.27	80.40	80.10
		(2.14)	(0.82)	(0.72)	(0.69)	(0.60)	(0.45)	(1.37)	(0.69)	(0.58)
	0.5 s	42.84	62.81	71.47	74.20	73.98	76.38	69.67	76.26	76.86
		(2.35)	(1.29)	(1.47)	(0.81)	(1.29)	(0.53)	(1.73)	(0.73)	(0.44)
CIFAR-100*	0.3 p	10.85	10.44	45.43	—	—	—	51.90	53.94	54.01
		(0.59)	(0.63)	(0.71)	—	—	—	(1.11)	(0.29)	(0.93)
	0.4 s	10.61	11.70	47.40	—	—	—	50.99	53.66	53.07
		(0.53)	(0.48)	(0.34)	—	—	—	(0.16)	(0.28)	(0.32)
	0.5 s	10.58	13.26	41.74	—	—	—	46.25	49.13	49.11
		(0.17)	(0.69)	(1.68)	—	—	—	(0.60)	(0.98)	(0.90)

* Note: “-F” methods for DIW are not applicable on CIFAR-100, since there are too few data in a class in a mini-batch.

We compared them under label noise and report the results in Table 6, where the “-F” or “-L” suffix means using the hidden-layer-output or loss-value transformation. In general, we can observe

- SIWs improve upon IW due to the introduction of FE;
- DIWs improve upon SIWs due to the dynamic nature of \mathcal{W} in DIWs;
- for DIWs with a pretrained FE (i.e., DIW1 and DIW3), updating the FE during training is usually better than fixing it throughout training;
- for DIWs whose FE is updated (i.e., DIW2 and DIW3), “-F” methods perform better when FE is pretrained, while “-L” methods do not necessarily need to pretrain FE.

Therefore, DIW2-L is more recommended, which was indeed used in the previous experiments.

Furthermore, we trained models on CIFAR-10 under 0.4 symmetric flip, projected 64-dimensional last-layer representations of training data by *t-distributed stochastic neighbor embedding* (t-SNE) [70], and visualized the embedded data in Figure 7. We can see that DIWs have more concentrated clusters of the embedded data, which implies the superiority of DIWs over IW and SIWs.

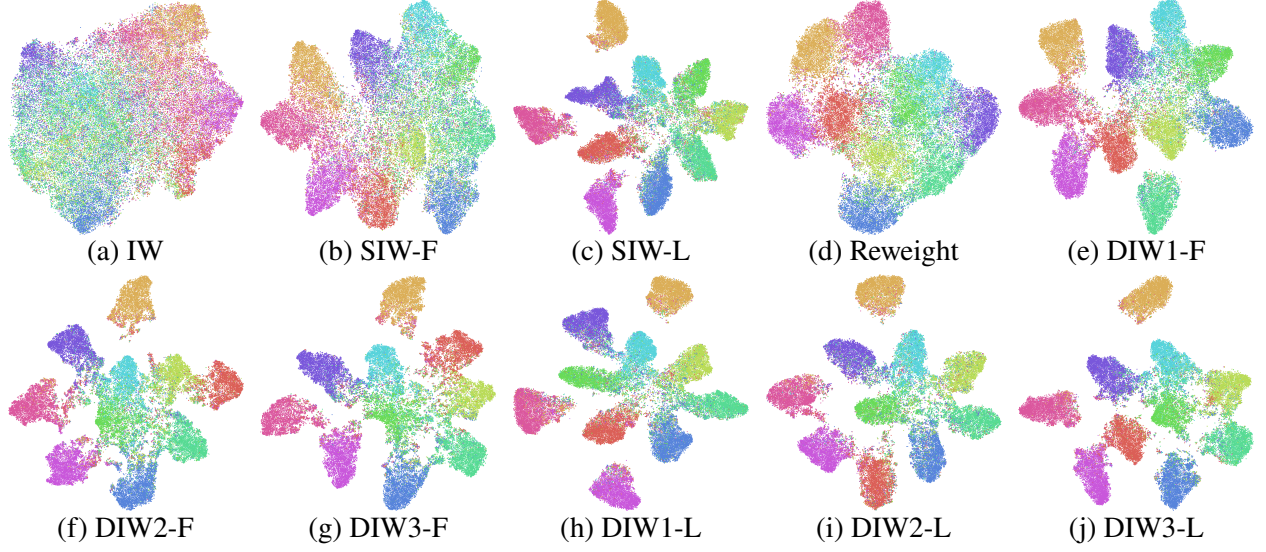


Figure 7: Visualizations of embedded data on noisy CIFAR-10 (colors mean ground-truth labels).

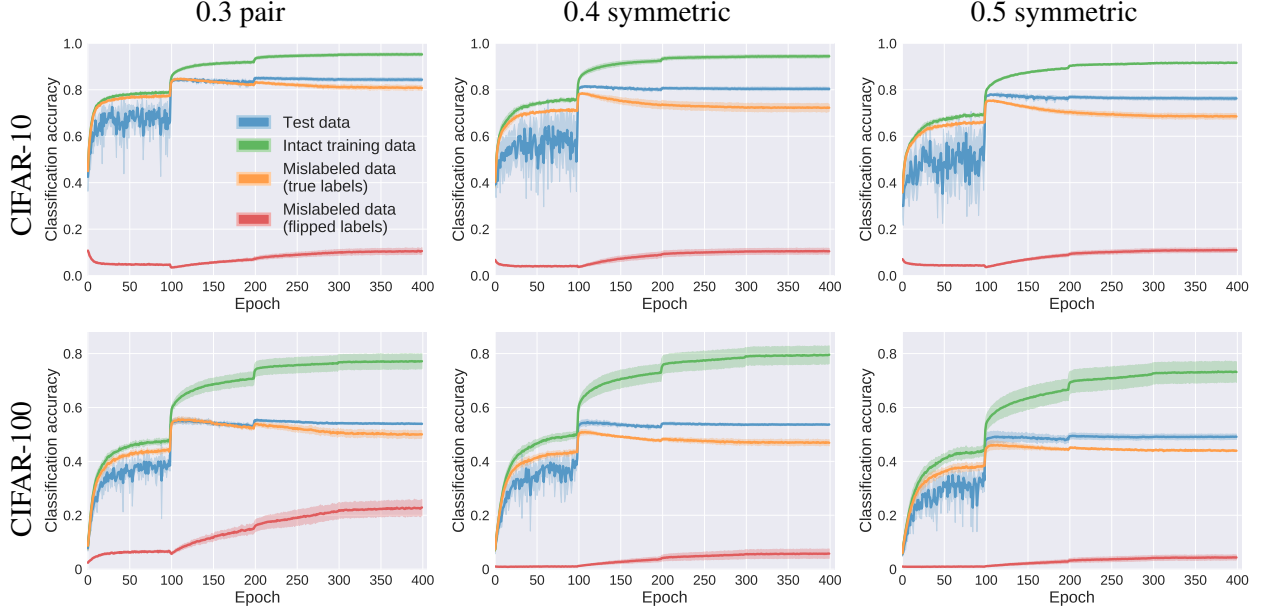


Figure 8: Denoising effect of DIW2-L on CIFAR-10/100 under label noise (5 trials).

Finally, we analyzed the denoising effect of DIW2-L on CIFAR-10/100 in Figure 8, by the curves of the training accuracy on the intact data, mislabeled data (evaluated by the flipped and ground-truth labels), and the test accuracy. According to Figure 8, DIW2-L can simultaneously fit the intact data and denoise the mislabeled data, so that for the mislabeled data, the flipped labels given for training correspond to much lower accuracy than the ground-truth labels withheld for training.

7 Causal Mechanism Transfer

In the *full-distribution shift* scenario, what can we use as a reasonable basis for transfer learning? In other words, what is a plausible *transfer assumption* that allows intricate shifts in the joint distributions between the source domains and the target domain? In this section, we explore the possibility of a causality-based foundation for transfer learning. Our motivation is simple: if we have different domains with the same causal mechanism that generates the data, it is plausible to think that one can exploit such a commonality of domains for transfer learning. However, the natural question is: how can we exploit such a commonality? We introduce the result of investigating this question, a novel method and foundation of transfer learning called *causal mechanism transfer* [71].

7.1 Motivation and Problem Setup

The problem setup we consider is that of the *independent component shift* scenario, a setting that emerges when the target and source distributions have a common causal mechanism behind them.

Such a common mechanism may be more conceivable in applications involving structured table data such as medical records [72]. For example, in medical record analysis for disease risk prediction, it can be reasonable to assume that there is a pathological mechanism that is common across regions or generations, but the data distributions may vary due to the difference in cultures or lifestyles. Such a hidden structure (pathological mechanism, in this case), once estimated, may provide portable knowledge to enable transfer learning, allowing one to obtain accurate predictors in under-investigated regions or for new generations.

7.1.1 Base Problem Setup

In this section, we consider a *multi-source few-shot supervised regression* transfer learning problem. Therefore, the output space is $\mathcal{Y} := \mathbb{R}$ (see Section 2.1). For notational brevity, we denote \mathbf{x} and y jointly as $\mathbf{z} = (\mathbf{x}, y) = (z^1, \dots, z^D)$ as well as $\mathcal{Z} = \mathbb{R}^D$, where $D = d_{\text{in}} + 1$.

Then, with some abuse of notation, we treat the loss function ℓ as a function over $\mathcal{F} \times \mathcal{Z}$ and write the true risk and empirical risk in (1) and (2) as

$$R(f) = \mathbb{E}_{(\mathbf{z}^{\text{te}}) \sim p_{\text{te}}(\mathbf{z})} \ell(f, \mathbf{z}^{\text{te}}),$$

$$\widehat{R}(f) = \frac{1}{n_{\text{tr}}} \sum_{i=1}^{n_{\text{tr}}} \ell(f, \mathbf{z}_i^{\text{tr}}).$$

Instead of a single source domain $p_{\text{tr}}(\mathbf{z})$, we assume that there are $K \geq 2$ source domains, and we have access to independent samples from these domains as $\{\mathcal{D}_k\}_{k \in [K]}$, where each $\mathcal{D}_k = \{\mathbf{z}_{k,i}^{\text{tr}}\}_{i=1}^{n_{\text{tr},k}}$ is a set of i.i.d. samples from $p_{\text{tr},k}(\mathbf{z})$.

We assume that we can access small data from the target domain, $\mathcal{D}_{\text{te}} = \{\mathbf{z}_j^{\text{te}}\}_{j=1}^{n_{\text{te}}}$, which is a set of i.i.d. samples from $p_{\text{te}}(\mathbf{z})$. We assume $n_{\text{te}}, n_{\text{tr},k} \geq D$ for simplicity.

The goal is to learn a predictor $f: \mathcal{X} \rightarrow \mathcal{Y}$ that minimizes the risk $R(f)$. Under this base problem setup, the question is what is the relation between the source domains and the target domain.

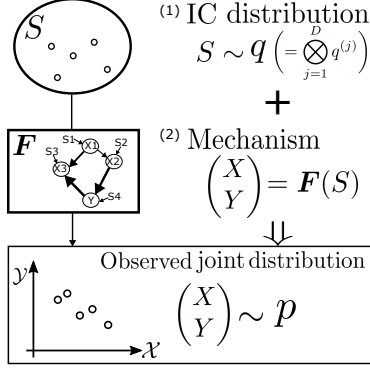


Figure 9: Nonparametric generative model of nonlinear independent component analysis. Our meta-distributional transfer assumption is built on the model, where there exists an invertible function \mathbf{F} representing the mechanism to generate labeled data (X, Y) from the independent components (ICs), S , sampled from q . As a result, each pair (\mathbf{F}, q) defines a joint density p .

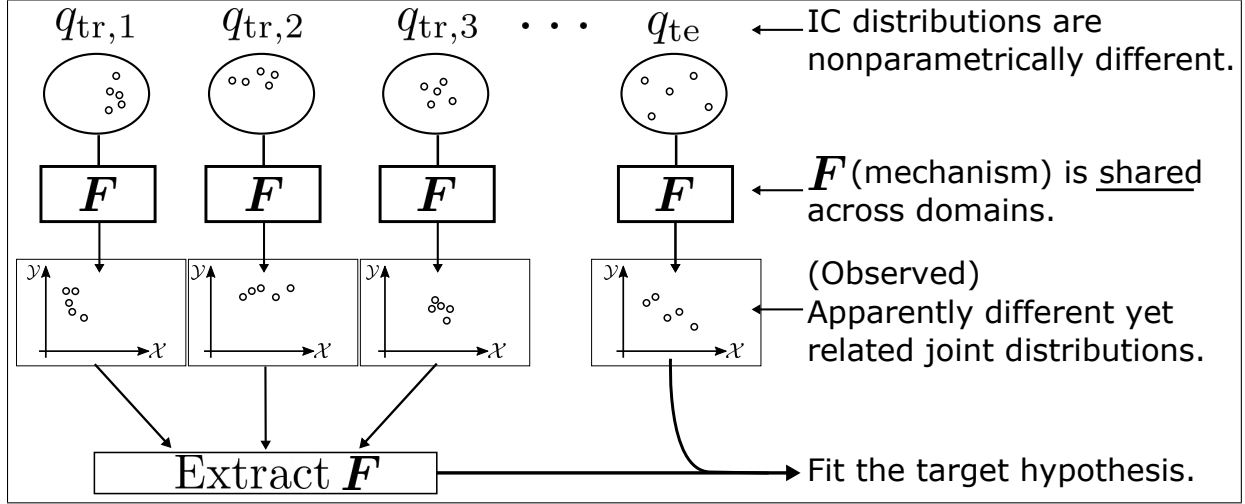


Figure 10: Our assumption of common generative mechanism. By capturing the common data generation mechanism, we enable domain adaptation among seemingly very different distributions without relying on parametric assumptions.

7.1.2 Key Assumption

Our key transfer assumption is that all domains follow nonlinear *independent component analysis* (ICA; e.g., [73]) models with identical mixing functions (Figure 10). Formally, the assumption is stated as follows (illustrated in Figures 9 and 10):

Assumption 1 (Main assumption [71]). *Let \mathcal{Q} be the set of the density (with respect to the Lebesgue measure) of independent distributions over \mathcal{Z} . We assume that there exists a set of independent component (IC) densities $q_{te}, q_{tr,k} \in \mathcal{Q} (k \in [K])$, and a smooth invertible function $\mathbf{F} : \mathbb{R}^D \rightarrow \mathbb{R}^D$ (the transformation or mixing map) such that $\mathbf{z}_{k,i}^{tr} \sim p_{tr,k}$ is generated by first sampling $S_{k,i}^{tr} \sim q_{tr,k}$ and later transforming it by*

$$\mathbf{z}_{k,i}^{tr} = \mathbf{F}(S_{k,i}^{tr}), \quad (22)$$

and similarly $\mathbf{z}_j^{te} = \mathbf{F}(S_j^{te}), S_j^{te} \sim q_{te}$ for p_{te} .

A salient example of generative models which results in (22) is *structural equation models* (SEMs; [74, 75]). More precisely, the generative model of (22) corresponds to the *reduced*

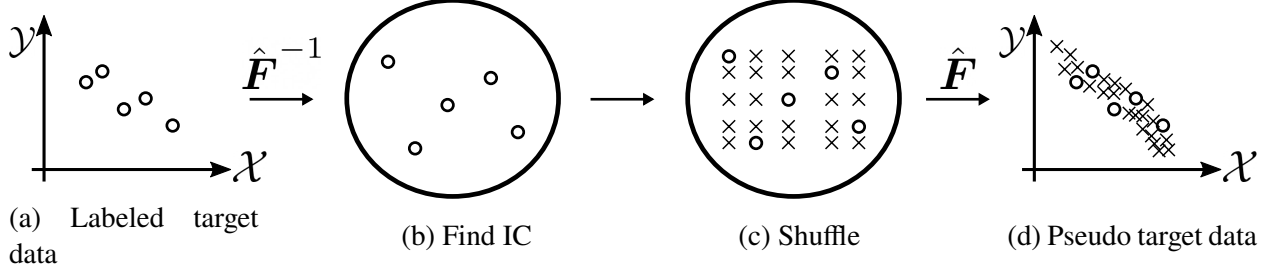


Figure 11: Schematic illustration of proposed few-shot domain adaptation method after estimating the common mechanism \mathbf{F} . With the estimated $\hat{\mathbf{F}}$, the method augments the small target domain sample in a few steps to enhance statistical efficiency: (a) The algorithm is given labeled target domain data. (b) From labeled target domain data, extract the ICs. (c) By shuffling the values, synthesize likely values of IC. (d) From the synthesized IC, generate pseudo target data. The generated data is used to fit a predictor for the target domain.

form [76] of a *Markovian* SEM [74], i.e., a form where the structural equations to determine Z from (Z, S) are solved so that Z is expressed as a function of S . Such a conversion is always possible because a Markovian SEM induces an *acyclic* causal graph [74], and hence the structural equations can be solved by elimination of variables. This interpretation of reduced-form SEMs as (22) has been exploited in methods of *causal discovery*, e.g., in the linear non-Gaussian additive-noise models and their successors [77, 78, 79]. In the case of SEMs, the key assumption of our method translates into the invariance of the causal mechanisms (expressed by the structural equations) across domains, which enables an intuitive assessment of the assumption based on prior knowledge. For instance, if all domains have the same causal mechanism and are in the same intervention state (including an intervention-free case), the modeling choice is deemed plausible. Note that we do not estimate the original structural equations in the proposed method, but we only require estimating the reduced form which is an easier problem compared to causal discovery, e.g., [80, 78, 79].

Under the assumption of invariant \mathbf{F} , since complex changes in q are allowed, intricate shifts in the apparent distribution p can be accommodated.

7.2 Causal Mechanism Transfer

Here, we detail the proposed method, causal mechanism transfer (Algorithm 4; [71]). The method proceeds in three steps: *estimation*, *inflation*, and *synthesis*, which are visually summarized in Figure 11.

7.2.1 Step 1: Estimation

First, we estimate the common generative mechanism \mathbf{F} , which is the sole connection between the source domains and the target domain. The estimation can be realized by performing nonlinear ICA using the source domain data, namely via *generalized contrastive learning* (GCL; [81]). GCL uses auxiliary information for training a certain binary classification function, $r_{\hat{\mathbf{F}}, \varphi}$, equipped with a parametrized feature extractor $\hat{\mathbf{F}} : \mathbb{R}^D \rightarrow \mathbb{R}^D$ and a set

of functions $\varphi = \{\varphi_j\}_{j=1}^D$, where each φ_j is a function from $\mathbb{R} \times \mathcal{U}$ to \mathbb{R} , and \mathcal{U} is some measurable space of auxiliary labels. The auxiliary information we use in our problem setup is the domain indices, and hence $\mathcal{U} = [K]$. The classification function to be trained in GCL is $r_{\hat{\mathbf{F}}, \varphi}(\mathbf{z}, u) := \sum_{j=1}^D \varphi_j((\hat{\mathbf{F}}^{-1}(\mathbf{z}))_j, u)$ consisting of $(\hat{\mathbf{F}}, \varphi)$, and the classification task of GCL is to classify (\mathbf{z}_k, k) as positive and (\mathbf{z}_k, k') ($k' \neq k$) as negative when $\mathbf{z}_k \in \mathcal{D}_k$. This yields the following domain-contrastive learning criterion to estimate \mathbf{F} :

$$\arg \min_{\hat{\mathbf{F}}, \{\varphi_j\}_{j=1}^D} \sum_{k=1}^K \frac{1}{n_{\text{tr}, k}} \sum_{i=1}^{n_{\text{tr}, k}} \left(\ell_{\log} \left(r_{\hat{\mathbf{F}}, \varphi}(\mathbf{z}_{k,i}^{\text{tr}}, k) \right) + \mathbb{E}_{k' \neq k} \ell_{\log} \left(-r_{\hat{\mathbf{F}}, \varphi}(\mathbf{z}_{k,i}^{\text{tr}}, k') \right) \right),$$

where $\mathbb{E}_{k' \neq k}$ denotes the expectation with respect to $k' \sim \text{Unif}([K] \setminus \{k\})$ (“Unif” denotes the uniform distribution), and ℓ_{\log} is the logistic loss $\ell_{\log}(m) := \log(1 + \exp(-m))$. The trained feature extractor $\hat{\mathbf{F}}$ is used as an estimator of \mathbf{F} . In experiments, $\hat{\mathbf{F}}$ is implemented by invertible neural networks [82], φ_j ($j \in [D]$) by multi-layer perceptron [6], and $\mathbb{E}_{k' \neq k}$ is replaced by a random sampling renewed for every mini-batch. Note that the invertible neural networks we use have been proven to be *universal approximators* for smooth invertible maps, which adds a layer of theoretical justification to the modeling choice [83].

7.2.2 Step 2: Inflation

Second, the method uses the estimated $\hat{\mathbf{F}}$ to perform data augmentation of the target domain data based on the knowledge transferred from the source domains. The second step extracts and inflates the target domain ICs using the estimated $\hat{\mathbf{F}}$. We first extract the ICs of the target domain data by applying the inverse of $\hat{\mathbf{F}}$ as

$$\hat{\mathbf{s}}_j = \hat{\mathbf{F}}^{-1}(\mathbf{z}_j^{\text{te}}).$$

After the extraction, we inflate the set of IC values by taking all dimension-wise combinations of the estimated IC:

$$\bar{\mathbf{s}}_{\mathbf{j}} = (\hat{s}_{j_1}^{(1)}, \dots, \hat{s}_{j_D}^{(D)}), \quad \mathbf{j} = (j_1, \dots, j_D) \in [n_{\text{te}}]^D,$$

to obtain new plausible IC values $\bar{\mathbf{s}}_{\mathbf{j}}$. The intuitive motivation of this procedure stems from the independence of the IC distributions. In our implementation, we used invertible neural networks [82] to model the function $\hat{\mathbf{F}}$ to enable the computation of the inverse $\hat{\mathbf{F}}^{-1}$.

7.2.3 Step 3: Synthesis

The third step estimates the target risk R by the empirical distribution of the augmented data:

$$\check{R}(f) := \frac{1}{n_{\text{te}}^D} \sum_{\mathbf{j} \in [n_{\text{te}}]^D} [\ell(f, \hat{\mathbf{F}}(\bar{\mathbf{s}}_{\mathbf{j}}))], \quad (23)$$

and performs empirical risk minimization. In experiments, we used a regularization term $\Omega(\cdot)$ to control the complexity of \mathcal{F} and selected

$$\hat{f} \in \arg \min_{f \in \mathcal{F}} \{\check{R}(f) + \Omega(f)\}.$$

Algorithm 4 Causal mechanism transfer.

Require: Source domain data sets $\{\mathcal{D}_k\}_{k \in [K]}$, target domain data set \mathcal{D}_{te} , nonlinear ICA algorithm ICA, and a learning algorithm $\mathcal{A}_{\mathcal{F}}$ to fit the hypothesis class \mathcal{F} of predictors.

// Step 1. Estimate the shared transformation.

$$\hat{\mathbf{F}} \leftarrow \text{ICA}(\mathcal{D}_1, \dots, \mathcal{D}_K)$$

// Step 2. Extract and shuffle target independent components

$$\hat{s}_j \leftarrow \hat{\mathbf{F}}^{-1}(z_j^{\text{te}}), \quad (j = 1, \dots, n_{\text{te}})$$

$$\{\bar{s}_{\mathbf{j}}\}_{\mathbf{j} \in [n_{\text{te}}]^D} \leftarrow \text{AllCombinations}(\{\hat{s}_j\}_{j=1}^{n_{\text{te}}})$$

// Step 3. Synthesize target data and fit the predictor.

$$\bar{z}_{\mathbf{j}} \leftarrow \hat{\mathbf{F}}(\bar{s}_{\mathbf{j}})$$

$$\hat{f} \leftarrow \mathcal{A}_{\mathcal{F}}(\{\bar{z}_{\mathbf{j}}\}_{\mathbf{j}})$$

Ensure: \hat{f} : the predictor in the target domain.

The generated hypothesis \hat{f} is then used to make predictions in the target domain. In our experiments, we used $\Omega(f) = \lambda \|f\|^2$, where $\lambda > 0$ and the norm is that of the reproducing kernel Hilbert space (RKHS) which we took the subset \mathcal{F} from. Note that we may well subsample only a subset of combinations in (23) to mitigate the computation cost similarly to [84] and [85].

7.3 Theoretical Insights

Next, we introduce the theoretical analysis of the proposed method. Since the proofs are involved and requires space, we omit the details here. We refer the interested readers to [71] and its supplementary material.

7.3.1 Complete-estimation Case: Minimum Variance Property

First, we consider the case that \mathbf{F} has been estimated perfectly. While this is an idealistic case, the analysis provides us with the intuition that the proposed method helps the learner in terms of the *variance* of the risk estimator.

Theorem 6 (Minimum variance property of \check{R}). *Assume that $\hat{\mathbf{F}} = \mathbf{F}$. Then, for each $f \in \mathcal{F}$, the proposed risk estimator $\check{R}(f)$ is the uniformly minimum variance unbiased estimator of $R(f)$, i.e., for any unbiased estimator $\tilde{R}(f)$ of $R(f)$,*

$$\forall q \in \mathcal{Q}, \quad \mathbb{V}(\check{R}(f)) \leq \mathbb{V}(\tilde{R}(f)),$$

where \mathbb{V} denotes the variance, and also $\mathbb{E}_{\text{te}} \check{R}(f) = R(f)$ holds where \mathbb{E}_{te} denotes the expectation with respect to p_{te} .

The proof of Theorem 6 is obtained by rewriting $R(f)$ as a D -variate *regular statistical functional* and $\check{R}(f)$ as its corresponding generalized U-statistic [86]. Theorem 6 implies that the proposed risk estimator can have superior statistical efficiency in terms of the variance over the ordinary empirical risk (2), since $\hat{R}(f)$ is also an unbiased estimator of $R(f)$.

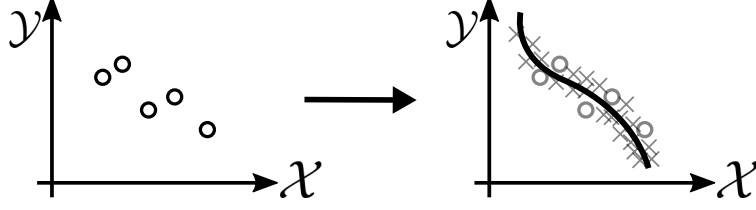


Figure 12: Fitting the data inflated by the proposed method. If the inflated data appear at the appropriate locations, the increment of the data has the effect of apparent complexity reduction since one can fit a complex predictor with less fear of overfitting. On the other hand, if the estimation of $\hat{\mathbf{F}}$ is poor, the fitting may be biased.

7.3.2 Incomplete-estimation Case: Excess Risk Bound

In real situations, one has to estimate \mathbf{F} . The following theorem characterizes the statistical gain and loss arising from the estimation error $\mathbf{F} - \hat{\mathbf{F}}$. The intuition is that the increased number of data points suppresses the possibility of overfitting because the hypothesis has to fit the majority of the inflated data (Figure 12) and not only the few original data, but the estimator $\hat{\mathbf{F}}$ has to be accurate so that fitting the inflated data is meaningful. Theorem 7 quantifies this consideration:

Theorem 7 (Excess risk bound). *Let \hat{f} be a minimizer of (23), and f^* be a minimizer of R (assuming both exist). Under appropriate assumptions (see Theorem 3 in the supplementary material of [71]), for arbitrary $\delta, \delta' \in (0, 1)$, we have with probability at least $1 - (\delta + \delta')$,*

$$\begin{aligned}
 R(\hat{f}) - R(f^*) \leq & \underbrace{C \sum_{j=1}^D \|\mathbf{F}_j - \hat{\mathbf{F}}_j\|_{W^{1,1}}}_{\text{Approximation error}} + \underbrace{4D\mathfrak{R}(\mathcal{F}) + 2DB_\ell \sqrt{\frac{\log 2/\delta}{2n_{\text{te}}}}}_{\text{Estimation error}} \\
 & + \underbrace{\zeta_1(\delta', n_{\text{te}}) + DB_\ell B_q \zeta_2(\mathbf{F} - \hat{\mathbf{F}})}_{\text{Higher order terms}}.
 \end{aligned}$$

Here, $\|\cdot\|_{W^{1,1}}$ is the $(1, 1)$ -Sobolev norm, and we define the effective Rademacher complexity $\mathfrak{R}(\mathcal{F})$ by

$$\mathfrak{R}(\mathcal{F}) := \frac{1}{n_{\text{te}}} \mathbb{E}_{\hat{s}} \mathbb{E}_{\sigma} \left[\sup_{f \in \mathcal{F}} \left| \sum_{j=1}^{n_{\text{te}}} \sigma_j \mathbb{E}_{S'_2, \dots, S'_D} [\tilde{\ell}(\hat{s}_j, S'_2, \dots, S'_D)] \right| \right],$$

where $\{\sigma_j\}_{j=1}^{n_{\text{te}}}$ are independent sign variables, $\mathbb{E}_{\hat{s}}$ is the expectation with respect to $\{\hat{s}_j\}_{j=1}^{n_{\text{te}}}$, the dummy variables S'_2, \dots, S'_D are i.i.d. copies of \hat{s}_1 , and $\tilde{\ell}$ is defined by using the degree- D symmetric group \mathfrak{S}_D as

$$\tilde{\ell}(s_1, \dots, s_D) := \frac{1}{D!} \sum_{\varsigma \in \mathfrak{S}_D} \ell(f, \hat{\mathbf{F}}(s_{\varsigma(1)}^{(1)}, \dots, s_{\varsigma(D)}^{(D)})),$$

and $\zeta_1(\delta', n)$ and $\zeta_2(\mathbf{F} - \hat{\mathbf{F}})$ are higher order terms. The constants B_q and B_ℓ depend only on q and ℓ , respectively, while C depends only on \mathbf{F} , q , ℓ , and D .

Details of the statement and the proof can be found in [71]. Note that the theorem is agnostic to how $\hat{\mathbf{F}}$ is obtained, hence it applies to more general problem setups as long as \mathbf{F} can be estimated. In Theorem 7, the utility of the proposed method appears in the effective complexity measure. The complexity is defined by a set of functions which are marginalized over all but one argument, resulting in mitigated dependence on the input dimensionality from exponential to linear (see Remark 3 in the supplementary material of [71] for details).

7.4 Experiments

Finally, we provide the results of proof-of-concept experiments to demonstrate the effectiveness of the proposed approach.

7.4.1 Datasets

We used the gasoline consumption data [87, p.284, Example 9.5], which is a panel data of gasoline usage in 18 of the OECD countries over 19 years. We considered each country as a domain, and we disregarded the time-series structure and considered the data as i.i.d. samples for each country in this proof-of-concept experiment. The dataset contains four variables, all of which were log-transformed: the motor gasoline consumption per car (the predicted variable), per-capita income, the motor gasoline price, and the stock of cars per capita (the predictor variables) [88]. The dataset has been used in econometric analyses involving SEMs [89], conforming to our approach.

7.4.2 Compared Methods

We compared the following transfer learning methods, all of which can be applied to regression problems. Unless explicitly specified, the predictor class \mathcal{F} was chosen to be kernel ridge regression (KRR; e.g., [5]) with the same hyperparameter candidates as the proposed method.

- Naive baselines (*SrcOnly*, *TarOnly*, and *S&TV*): *SrcOnly* (resp. *TarOnly*) trains a predictor on the source domain data (resp. target training data) without any device. *SrcOnly* can be effective if the source domains and the target domain have highly similar distributions. The *S&TV* baseline trains on both source and target domain data, but the LOOCV score is computed only from the target domain data.
- *TrAdaBoost*: Two-stage TrAdaBoost.R2; a boosting method tailored for few-shot regression transfer proposed in [90]. It is an iterative method with early-stopping [90], for which we used the leave-one-out cross-validation score on the target domain data as the criterion. As suggested in [90], we set the maximum number of outer loop iterations at 30. The base predictor is the decision tree regressor with the maximum depth 6 [6]. Note that although TrAdaBoost does not have a clarified transfer assumption, we compared the performance for reference.
- *IW*: Importance-weighted KRR using RuLSIF [27] (see also Section 4.2). The method directly estimates a relative joint density ratio function $\frac{p_{te}(\mathbf{z})}{\alpha p_{te}(\mathbf{z}) + (1-\alpha)p_{tr}(\mathbf{z})}$ for $\alpha \in [0, 1)$, where p_{tr} is a hypothetical source distribution created by pooling all source domain data. Following [27], we experimented on $\alpha \in \{0, 0.5, 0.95\}$ and reported the results of 0.5

which performed the best among the three. The regularization coefficient λ' was selected from $\lambda' \in 2^{\{-10, \dots, 10\}}$ using importance-weighted cross-validation [16].

- **GDM:** Generalized discrepancy minimization [91]. This method performs instance-weighted training on the source domain data with the weights that minimize the *generalized discrepancy* (via quadratic programming). We selected the hyperparameters λ_r from $2^{\{-10, \dots, 10\}}$ as suggested in [91]. The selection criterion is the performance of the trained predictor on the target training data as the method trains on the source domain data and the target unlabeled data.
- **Copula:** The non-parametric regular-vine copula method [92]. This method presumes to use a specific joint density estimator called regular-vine (R-vine) copulas. Adaptation is realized in two steps: the first step estimates which components of the constructed R-vine model are different by performing two-sample tests based on maximum mean discrepancy [92], and the second step re-estimates the components in which a change is detected using only the target domain data.
- **LOO** (reference score): The leave-one-out cross-validated error estimate was also calculated for reference. It is the average prediction error for a single held-out test point when the predictor is trained on the rest of the target domain data.

Evaluation Procedure The prediction accuracy was measured by the mean squared error (MSE). For each train-test split, we randomly selected one-third (6 points) of the target domain dataset as the training set and use the rest as the test set. All experiments were repeated 10 times with different train-test splits of target domain data.

Configuration of the Proposed Method We modeled $\hat{\mathbf{F}}$ by an 8-layer Glow neural network [82]. We modeled φ_j by a 1-hidden-layer neural network with a varied number of hidden units, K output units, and the rectified linear unit activation [93]. We used its k -th output ($k \in [K]$) as the value for $\varphi_j(\cdot, k)$. For training, we use the Adam optimizer [67] with fixed parameters $(\beta_1, \beta_2, \epsilon) = (0.9, 0.999, 10^{-8})$, fixed initial learning rate 10^{-3} , and the maximum number of epochs 300. For further implementation details, see [71]. For each evaluation step, we took all combinations (with replacement) of the estimated ICs to synthesize target domain data. After we synthesized the data, we filtered them by applying a novelty detection technique with respect to the union of source domain data, namely the *one-class support vector machine* [5] with the fixed parameter $\nu = 0.1$ and radial basis function (RBF; e.g., [5]) kernel $k(x, y) = \exp(-\|x - y\|^2/\gamma)$ with $\gamma = D$. This is because the estimated transform $\hat{\mathbf{F}}$ is not expected to be trained well outside the union of the supports of the source distributions. After performing the filtration, we combined the original target training data with the augmented data to ensure the original data points to be always included.

Predictor Hypothesis Class \mathcal{F} As the predictor model, we used the KRR with the RBF kernel. The bandwidth γ was chosen by the median heuristic similarly to [27] for simplicity. Note that the choice of the predictor model is for the sake of comparison with the other methods tailored for KRR [91], and that an arbitrary predictor hypothesis class and learning algorithm can be easily combined with the proposed approach.

Hyperparameter Selection We performed grid-search for hyperparameter selection. The number of hidden units for φ_j was chosen from $\{10, 20\}$ and the coefficient of weight-decay from $10^{\{-2, -1\}}$. The ℓ_2 -regularization coefficient λ of KRR was chosen from $\lambda \in 2^{\{-10, \dots, 10\}}$ following [91]. To perform hyperparameter selection as well as early-stopping, we recorded

the leave-one-out cross-validation (LOOCV) mean-squared error on the target training data every 20 epochs and selected its minimizer. The leave-one-out score was computed using the well-known closed-form formula instead of training the predictor for each split [94]. Note that we only used the original target domain data as the held-out set and not the synthesized data.

7.4.3 Experimental Results

In Table 7, we report the MSE scores normalized by that of *LOO* to facilitate the comparison, similarly to [95].

In many of the target domain choices, the naive baselines (*SrcOnly* and *S&TV*) suffered from negative transfer, i.e., higher average MSEs than *TarOnly* (in 12 out of 18 domains). On the other hand, the proposed method performed better than *TarOnly* or was more resistant to negative transfer than the other compared methods. The performances of *GDM*, *Copula*, and *IW* were often inferior even compared to the baseline performance of *SrcAndTarValid*. For *GDM* and *IW*, this was attributed to the fact that these methods presume the availability of abundant (unlabeled) target domain data, which was unavailable in the current problem setup. For *Copula*, the performance inferior to the naive baselines was possibly due to the restriction of the predictor model to its accompanied probability model [92]. *TrAdaBoost* worked reasonably well for many but not all domains. For some domains, it suffered from negative transfer similarly to others, possibly because of the very small number of training data points. Note that the transfer assumption of *TrAdaBoost* has not been stated [90], and it is not clear when the method is reliable.

The domains on which the baselines perform better than the proposed method can be explained by the following two cases: (i) easier domains allow naive baselines to perform well and (ii) some domains may have deviated \mathbf{F} . Case (i) implies that estimating \mathbf{F} is unnecessary, and hence the proposed method can be suboptimal (more likely for JPN, NLD, NOR, and SWE in Table 7, where *SrcOnly* or *S&TV* improved upon *TrgOnly*). On the other hand, case (ii) implies that an approximation error was induced as in Theorem 7 (more likely for IRL and ITA in Table 7). In this case, others also perform poorly, implying the difficulty of the problem instance. In either case, in practice, one may well perform cross-validation to fall back into the baselines.

8 Conclusion

In this article, we rethought classical importance-weighting based approaches for transfer learning and explained their limitations on the two-step architecture: as data nowadays are becoming more and more complex and high-dimensional, the first importance estimation step can be very difficult and the resulted estimation error will propagate to the second weighted training step, degrading the prediction performance of the trained model.

To avoid the issue, we introduced two one-step solutions: one learns an importance estimator and a predictor jointly by minimizing an upper bound of the test risk, and the other iterates weight estimation and weighted training with features for weight estimation extracted as hidden-layer outputs or loss values. Furthermore, we presented a transfer learning method built upon the common data generation causal mechanism.

Table 7: Results of the real-world data experiments for different choices of the target domain. The evaluation score was MSE normalized by that of *LOO* (the lower the better). All experiments were repeated 10 times with different train-test splits of target domain data, and the average performance is reported with the standard errors in the brackets. The target column indicates abbreviated country names. Bold-face indicates the best score (Prop: proposed method, TrAda: *TrAdaBoost*, the numbers in the brackets of IW indicate the value of α). The proposed method often improved upon the baseline *TarOnly* or was relatively more resistant to negative transfer, with notable improvements in *DEU*, *GBR*, and *USA*.

Target	(LOO)	TarOnly	Prop	SrcOnly	S&TV	TrAda	GDM	Copula	IW(.5)
AUT	1	5.88 (1.60)	5.39 (1.86)	9.67 (0.57)	9.84 (0.62)	5.78 (2.15)	31.56 (1.39)	27.33 (0.77)	34.06 (0.67)
BEL	1	10.70 (7.50)	7.94 (2.19)	8.19 (0.68)	9.48 (0.91)	8.10 (1.88)	89.10 (4.12)	119.86 (2.64)	105.68 (3.13)
CAN	1	5.16 (1.36)	3.84 (0.98)	157.74 (8.83)	156.65 (10.69)	51.94 (30.06)	516.90 (4.45)	406.91 (1.59)	571.33 (1.60)
DNK	1	3.26 (0.61)	3.23 (0.63)	30.79 (0.93)	28.12 (1.67)	25.60 (13.11)	16.84 (0.85)	14.46 (0.79)	21.83 (0.93)
FRA	1	2.79 (1.10)	1.92 (0.66)	4.67 (0.41)	3.05 (0.11)	52.65 (25.83)	91.69 (1.34)	156.29 (1.96)	113.5 (1.15)
DEU	1	16.99 (8.04)	6.71 (1.23)	229.65 (9.13)	210.59 (14.99)	341.03 (157.80)	739.29 (11.81)	929.03 (4.85)	807.88 (4.14)
GRC	1	3.80 (2.21)	3.55 (1.79)	5.30 (0.90)	5.75 (0.68)	11.78 (2.36)	26.90 (1.89)	23.05 (0.53)	39.56 (1.70)
IRL	1	3.05 (0.34)	4.35 (1.25)	135.57 (5.64)	12.34 (0.58)	23.40 (17.50)	3.84 (0.22)	26.60 (0.59)	5.79 (0.12)
ITA	1	13.00 (4.15)	14.05 (4.81)	35.29 (1.83)	39.27 (2.52)	87.34 (24.05)	226.95 (11.14)	343.10 (10.04)	237.15 (6.46)
JPN	1	10.55 (4.67)	12.32 (4.95)	8.10 (1.05)	8.38 (1.07)	18.81 (4.59)	95.58 (7.89)	71.02 (5.08)	129.3 (10.47)
NLD	1	3.75 (0.80)	3.87 (0.79)	0.99 (0.06)	0.99 (0.05)	9.45 (1.43)	28.35 (1.62)	29.53 (1.58)	33.38 (1.63)
NOR	1	2.70 (0.51)	2.82 (0.73)	1.86 (0.29)	1.63 (0.11)	24.25 (12.50)	23.36 (0.88)	31.37 (1.17)	27.09 (0.76)
ESP	1	5.18 (1.05)	6.09 (1.53)	5.17 (1.14)	4.29 (0.72)	14.85 (4.20)	33.16 (6.99)	152.59 (6.19)	56.54 (2.16)
SWE	1	6.44 (2.66)	5.47 (2.63)	2.48 (0.23)	2.02 (0.21)	2.18 (0.25)	15.53 (2.59)	2706.85 (17.91)	113.55 (1.72)
CHE	1	3.51 (0.46)	2.90 (0.37)	43.59 (1.77)	7.48 (0.49)	38.32 (9.03)	8.43 (0.24)	29.71 (0.53)	9.33 (0.22)
TUR	1	1.65 (0.47)	1.06 (0.15)	1.22 (0.18)	0.91 (0.09)	2.19 (0.34)	64.26 (5.71)	142.84 (2.04)	139.29 (2.41)
GBR	1	5.95 (1.86)	2.66 (0.57)	15.92 (1.02)	10.05 (1.47)	7.57 (5.10)	50.04 (1.75)	68.70 (1.25)	69.19 (0.87)
USA	1	4.98 (1.96)	1.60 (0.42)	21.53 (3.30)	12.28 (2.52)	2.06 (0.47)	308.69 (5.20)	244.90 (1.82)	393.45 (1.68)
#Best	-	2	10	2	4	0	0	0	0

Future work will consider adapting the proposed methods to evolving domain shift in non-stationary environments [96, 97], and study other meta-distributional concepts for capturing the intrinsic structure of the evolving domain data. From the practical application viewpoint, we will employ the one-step importance-weighting techniques for deep reinforcement learning where the agents may face some visual changes [98], and use the novel causal mechanism transfer learning method in health data across different population groups [99].

Acknowledgments

NL, TF, and MS were supported by the Institute for AI and Beyond, UTokyo. MS was also supported by JST AIP Acceleration Research Grant Number JPMJCR20U3, Japan. TZ and TF were supported by the SPRING GX program at UTokyo. TT was supported by RIKEN Junior Research Associate Program and Masason Foundation.

References

- [1] I. Goodfellow, Y. Bengio, and A. Courville, *Deep learning*. MIT Press, 2016.
- [2] G. Wahba, *Spline Models for Observational Data*, vol. 59. SIAM, 1990.
- [3] C. M. Bishop, *Neural Networks for Pattern Recognition*. Oxford University Press, 1995.
- [4] V. N. Vapnik, *Statistical Learning Theory*. Wiley-Interscience, 1998.
- [5] B. Schölkopf and A. J. Smola, *Learning with Kernels: Support Vector Machines, Regularization, Optimization, and Beyond*. MIT Press, 2001.
- [6] T. Hastie, R. Tibshirani, and J. Friedman, *The Elements of Statistical Learning: Data mining, Inference, and Prediction*. Springer Science & Business Media, 2009.
- [7] R. O. Duda, P. E. Hart, and D. G. Stork, *Pattern Classification*. John Wiley & Sons, 2012.
- [8] M. Sugiyama, *Introduction to Statistical Machine Learning*. Morgan Kaufmann, 2015.
- [9] F. Yu, H. Chen, X. Wang, W. Xian, Y. Chen, F. Liu, V. Madhavan, and T. Darrell, “Bdd100k: A diverse driving dataset for heterogeneous multitask learning,” in *Proceedings of the IEEE/CVF conference on computer vision and pattern recognition*, pp. 2636–2645, 2020.
- [10] P. W. Koh, S. Sagawa, S. M. Xie, M. Zhang, A. Balsubramani, W. Hu, M. Yasunaga, R. L. Phillips, I. Gao, T. Lee, *et al.*, “Wilds: A benchmark of in-the-wild distribution shifts,” in *Proceedings of International Conference on Machine Learning*, pp. 5637–5664, 2021.
- [11] R. A. Berk, “An introduction to sample selection bias in sociological data,” *American Sociological Review*, pp. 386–398, 1983.
- [12] B. Zadrozny, “Learning and evaluating classifiers under sample selection bias,” in *Proceedings of International Conference on Machine Learning*, pp. 903–910, 2004.

- [13] B. van Rooyen and R. C. Williamson, “A theory of learning with corrupted labels,” *Journal of Machine Learning Research*, vol. 18, no. 228, pp. 1–50, 2018.
- [14] B. Han, Q. Yao, T. Liu, G. Niu, I. W. Tsang, J. T. Kwok, and M. Sugiyama, “A survey of label-noise representation learning: Past, present and future,” *Preprint arXiv:2011.04406*, 2020.
- [15] J. Quionero-Candela, M. Sugiyama, A. Schwaighofer, and N. D. Lawrence, *Dataset Shift in Machine Learning*. MIT Press, 2009.
- [16] M. Sugiyama and M. Kawanabe, *Machine Learning in Non-stationary Environments: Introduction to Covariate Shift Adaptation*. MIT Press, 2012.
- [17] W. G. Cochran, *Sampling Techniques*. John Wiley & Sons, 2007.
- [18] G. Fishman, *Monte Carlo: Concepts, Algorithms, and Applications*. Springer Science & Business Media, 2013.
- [19] H. Kahn and A. W. Marshall, “Methods of reducing sample size in Monte Carlo computations,” *Journal of the Operations Research Society of America*, vol. 1, no. 5, pp. 263–278, 1953.
- [20] H. Shimodaira, “Improving predictive inference under covariate shift by weighting the log-likelihood function,” *Journal of Statistical Planning and Inference*, vol. 90, no. 2, pp. 227–244, 2000.
- [21] M. Sugiyama and K.-R. Müller, “Input-dependent estimation of generalization error under covariate shift,” *Statistics & Decisions*, vol. 23, no. 4, pp. 249–279, 2005.
- [22] M. Sugiyama, M. Krauledat, and K.-R. Müller, “Covariate shift adaptation by importance weighted cross validation,” *Journal of Machine Learning Research*, vol. 8, no. 5, pp. 985–1005, 2007.
- [23] J. Huang, A. Gretton, K. Borgwardt, B. Schölkopf, and A. J. Smola, “Correcting sample selection bias by unlabeled data,” in *Advances in Neural Information Processing Systems 19*, pp. 601–608, 2007.
- [24] M. Sugiyama, S. Nakajima, H. Kashima, P. v. Buenau, and M. Kawanabe, “Direct importance estimation with model selection and its application to covariate shift adaptation,” in *Advances in Neural Information Processing Systems 20*, pp. 1433–1440, 2008.
- [25] M. Sugiyama, T. Suzuki, S. Nakajima, H. Kashima, P. von Büna, and M. Kawanabe, “Direct importance estimation for covariate shift adaptation,” *Annals of the Institute of Statistical Mathematics*, vol. 60, no. 4, pp. 699–746, 2008.
- [26] T. Kanamori, S. Hido, and M. Sugiyama, “A least-squares approach to direct importance estimation,” *Journal of Machine Learning Research*, vol. 10, no. 7, pp. 1391–1445, 2009.

- [27] M. Yamada, T. Suzuki, T. Kanamori, H. Hachiya, and M. Sugiyama, “Relative density-ratio estimation for robust distribution comparison,” in *Advances in Neural Information Processing Systems 24*, pp. 594–602, 2011.
- [28] M. Sugiyama, T. Suzuki, and T. Kanamori, *Density Ratio Estimation in Machine Learning*. Cambridge University Press, 2012.
- [29] K. Zhang, B. Schölkopf, K. Muandet, and Z. Wang, “Domain adaptation under target and conditional shift,” in *Proceedings of International Conference on Machine Learning*, pp. 819–827, 2013.
- [30] T. Zhang, I. Yamane, N. Lu, and M. Sugiyama, “A one-step approach to covariate shift adaptation,” in *Proceedings of Asian Conference on Machine Learning*, pp. 65–80, 2020.
- [31] T. Zhang, I. Yamane, N. Lu, and M. Sugiyama, “A one-step approach to covariate shift adaptation,” *SN Computer Science*, vol. 2, no. 4, pp. 1–12, 2021.
- [32] S. Ben-David, N. Eiron, and P. M. Longc, “On the difficulty of approximately maximizing agreements,” *Journal of Computer and System Sciences*, vol. 66, no. 3, pp. 496–514, 2003.
- [33] P. L. Bartlett, M. I. Jordan, and J. D. McAuliffe, “Convexity, classification, and risk bounds,” *Journal of the American Statistical Association*, vol. 101, no. 473, pp. 138–156, 2006.
- [34] S. J. Pan and Q. Yang, “A survey on transfer learning,” *IEEE Transactions on Knowledge and Data Engineering*, vol. 22, no. 10, pp. 1345–1359, 2009.
- [35] Q. Yang, Y. Zhang, W. Dai, and S. J. Pan, *Transfer Learning*. Cambridge University Press, 2020.
- [36] D. Angluin and P. Laird, “Learning from noisy examples,” *Machine Learning*, vol. 2, no. 4, pp. 343–370, 1988.
- [37] C. Zhang, S. Bengio, M. Hardt, B. Recht, and O. Vinyals, “Understanding deep learning requires rethinking generalization,” in *Proceedings of International Conference on Learning Representations*, 2017.
- [38] N. Japkowicz and S. Stephen, “The class imbalance problem: A systematic study,” *Intelligent Data Analysis*, vol. 6, no. 5, pp. 429–449, 2002.
- [39] H. He and E. A. Garcia, “Learning from imbalanced data,” *IEEE Transactions on Knowledge and Data Engineering*, vol. 21, no. 9, pp. 1263–1284, 2009.
- [40] C. Huang, Y. Li, C. Change Loy, and X. Tang, “Learning deep representation for imbalanced classification,” in *Proceedings of IEEE Conference on Computer Vision and Pattern Recognition*, pp. 5375–5384, 2016.
- [41] M. Buda, A. Maki, and M. A. Mazurowski, “A systematic study of the class imbalance problem in convolutional neural networks,” *Neural Networks*, vol. 106, pp. 249–259, 2018.

- [42] Z. C. Lipton, Y.-X. Wang, and A. Smola, “Detecting and correcting for label shift with black box predictors,” in *Proceedings of International Conference on Machine Learning*, pp. 3128–3136, 2018.
- [43] K. Cao, C. Wei, A. Gaidon, N. Arechiga, and T. Ma, “Learning imbalanced datasets with label-distribution-aware margin loss,” in *Advances in Neural Information Processing Systems 32*, pp. 1565–1576, 2019.
- [44] M. Gong, K. Zhang, T. Liu, D. Tao, C. Glymour, and B. Schölkopf, “Domain adaptation with conditional transferable components,” in *Proceedings of International Conference on Machine Learning*, pp. 2839–2848, 2016.
- [45] X. Yu, T. Liu, M. Gong, K. Zhang, K. Batmanghelich, and D. Tao, “Label-noise robust domain adaptation,” in *International Conference on Machine Learning*, pp. 10913–10924, 2020.
- [46] T. Fang, N. Lu, G. Niu, and M. Sugiyama, “Rethinking importance weighting for deep learning under distribution shift,” in *Advances in Neural Information Processing Systems 33*, pp. 11996–12007, 2020.
- [47] N. Cristianini and J. Shawe-Taylor, *An Introduction to Support Vector Machines: And Other Kernel-Based Learning Methods*. Cambridge University Press, 1999.
- [48] A. E. Beaton and J. W. Tukey, “The fitting of power series, meaning polynomials, illustrated on band-spectroscopic data,” *Technometrics*, vol. 16, no. 2, pp. 147–185, 1974.
- [49] R. Andersen, *Modern Methods for Robust Regression*, vol. 152. SAGE, 2008.
- [50] H. Robbins and S. Monro, “A stochastic approximation method,” *The Annals of Mathematical Statistics*, pp. 400–407, 1951.
- [51] X. Yang, Q. Song, and Y. Wang, “A weighted support vector machine for data classification,” *International Journal of Pattern Recognition and Artificial Intelligence*, vol. 21, no. 5, pp. 961–976, 2007.
- [52] V. Koltchinskii, “Rademacher penalties and structural risk minimization,” *IEEE Transactions on Information Theory*, vol. 47, no. 5, pp. 1902–1914, 2001.
- [53] M. Mohri, A. Rostamizadeh, and A. Talwalkar, *Foundations of Machine Learning*. MIT Press, 2018.
- [54] S. Shalev-Shwartz and S. Ben-David, *Understanding Machine Learning: From Theory to Algorithms*. Cambridge University Press, 2014.
- [55] C. F. Ahmed, N. Lachiche, C. Charnay, and A. Braud, “Dataset shift in a real-life dataset,” in *ECML-PKDD Workshop on Learning over Multiple Contexts*, 2014.
- [56] X. Chen, M. Monfort, A. Liu, and B. D. Ziebart, “Robust covariate shift regression,” in *Proceedings of International Conference on Artificial Intelligence and Statistics*, pp. 1270–1279, 2016.

- [57] A. J. Storkey and M. Sugiyama, “Mixture regression for covariate shift,” in *Advances in Neural Information Processing Systems 19*, pp. 1337–1344, 2007.
- [58] C. Cortes, M. Mohri, M. Riley, and A. Rostamizadeh, “Sample selection bias correction theory,” in *Proceedings of International Conference on Algorithmic Learning Theory*, pp. 38–53, Springer, 2008.
- [59] H. Xiao, K. Rasul, and R. Vollgraf, “Fashion-MNIST: A novel image dataset for benchmarking machine learning algorithms,” *Preprint arXiv:1708.07747v2*, 2017.
- [60] T. Clanuwat, M. Bober-Irizar, A. Kitamoto, A. Lamb, K. Yamamoto, and D. Ha, “Deep learning for classical Japanese literature,” *arXiv preprint arXiv:1812.01718*, 2018.
- [61] J. Byrd and Z. C. Lipton, “What is the effect of importance weighting in deep learning?,” in *International Conference on Machine Learning*, pp. 872–881, 2019.
- [62] N. Srivastava, G. Hinton, A. Krizhevsky, I. Sutskever, and R. Salakhutdinov, “Dropout: A simple way to prevent neural networks from overfitting,” *Journal of Machine Learning Research*, vol. 15, no. 1, pp. 1929–1958, 2014.
- [63] M. Ren, W. Zeng, B. Yang, and R. Urtasun, “Learning to reweight examples for robust deep learning,” in *Proceedings of International Conference on Machine Learning*, pp. 4334–4343, 2018.
- [64] A. Krizhevsky and G. Hinton, “Learning multiple layers of features from tiny images,” tech. rep., 2009. <https://www.cs.toronto.edu/~kriz/learning-features-2009-TR.pdf>.
- [65] Y. LeCun, L. Bottou, Y. Bengio, and P. Haffner, “Gradient-based learning applied to document recognition,” *Proceedings of the IEEE*, vol. 86, no. 11, pp. 2278–2324, 1998.
- [66] K. He, X. Zhang, S. Ren, and J. Sun, “Deep residual learning for image recognition,” in *In Proceedings of IEEE Conference on Computer Vision and Pattern Recognition*, pp. 770–778, 2016.
- [67] D. P. Kingma and J. L. Ba, “Adam: A method for stochastic optimization,” in *Proceedings of International Conference on Learning Representations*, 2015.
- [68] B. Han, Q. Yao, X. Yu, G. Niu, M. Xu, W. Hu, I. Tsang, and M. Sugiyama, “Co-teaching: Robust training of deep neural networks with extremely noisy labels,” in *Advances in Neural Information Processing Systems 31*, pp. 8527–8537, 2018.
- [69] B. Van Rooyen, A. Menon, and R. C. Williamson, “Learning with symmetric label noise: The importance of being unhinged,” in *Advances in Neural Information Processing Systems 28*, pp. 10–18, 2015.
- [70] L. van der Maaten and G. Hinton, “Visualizing data using t-SNE,” *Journal of Machine Learning Research*, vol. 9, no. Nov, pp. 2579–2605, 2008.

- [71] T. Teshima, I. Sato, and M. Sugiyama, “Few-shot domain adaptation by causal mechanism transfer,” in *Proceedings of International Conference on Machine Learning*, pp. 9458–9469, 2020.
- [72] P. Yadav, M. Steinbach, V. Kumar, and G. Simon, “Mining electronic health records (EHRs): A survey,” *ACM Computing Surveys*, vol. 50, no. 6, pp. 1–40, 2018.
- [73] A. Hyvärinen, J. Karhunen, and E. Oja, *Independent Component Analysis*. John Wiley & Sons, Inc., 2001.
- [74] J. Pearl, *Causality: Models, Reasoning and Inference*. Cambridge University Press, second ed., 2009.
- [75] J. Peters, D. Janzing, and B. Schölkopf, *Elements of Causal Inference: Foundations and Learning Algorithms*. MIT Press, 2017.
- [76] P. C. Reiss and F. A. Wolak, “Structural econometric modeling: Rationales and examples from industrial organization,” in *Handbook of Econometrics*, vol. 6, pp. 4277–4415, Elsevier, 2007.
- [77] Y. Kano and S. Shimizu, “Causal inference using nonnormality,” in *Proceedings of the International Symposium on the Science of Modeling, the 30th Anniversary of the Information Criterion*, pp. 261–270, 2003.
- [78] S. Shimizu, P. O. Hoyer, A. Hyvärinen, and A. J. Kerminen, “A linear non-Gaussian acyclic model for causal discovery,” *Journal of Machine Learning Research*, vol. 7, no. 72, pp. 2003–2030, 2006.
- [79] R. P. Monti, K. Zhang, and A. Hyvärinen, “Causal discovery with general non-linear relationships using non-linear ICA,” in *Proceedings of Conference on Uncertainty in Artificial Intelligence*, pp. 186–195, 2019.
- [80] C. Glymour, K. Zhang, and P. Spirtes, “Review of Causal Discovery Methods Based on Graphical Models,” *Frontiers in Genetics*, vol. 10, no. 524, 2019.
- [81] A. Hyvärinen, H. Sasaki, and R. Turner, “Nonlinear ICA using auxiliary variables and generalized contrastive learning,” in *Proceedings of International Conference on Artificial Intelligence and Statistics*, pp. 859–868, 2019.
- [82] D. P. Kingma and P. Dhariwal, “Glow: Generative flow with invertible 1x1 convolutions,” in *Advances in Neural Information Processing Systems 31*, pp. 10215–10224, 2018.
- [83] T. Teshima, I. Ishikawa, K. Tojo, K. Oono, M. Ikeda, and M. Sugiyama, “Coupling-based invertible neural networks are universal diffeomorphism approximators,” in *Advances in Neural Information Processing Systems 33*, pp. 3362–3373, 2020.
- [84] S. Cléménçon, I. Colin, and A. Bellet, “Scaling-up empirical risk minimization: Optimization of incomplete U-statistics,” *Journal of Machine Learning Research*, vol. 17, no. 76, pp. 1–36, 2016.

- [85] G. Papa, S. Cléménçon, and A. Bellet, “SGD algorithms based on incomplete U-statistics: Large-scale minimization of empirical risk,” in *Advances in Neural Information Processing Systems* 28, pp. 1027–1035, 2015.
- [86] A. J. Lee, *U-Statistics: Theory and Practice*. M. Dekker, 1990.
- [87] W. H. Greene, *Econometric Analysis*. Prentice Hall, seventh ed., 2012.
- [88] B. H. Baltagi and J. M. Griffin, “Gasoline demand in the OECD: An application of pooling and testing procedures,” *European Economic Review*, vol. 22, no. 2, pp. 117–137, 1983.
- [89] B. Baltagi, *Econometric Analysis of Panel Data*. John Wiley and Sons, 3rd ed., 2005.
- [90] D. Pardoe and P. Stone, “Boosting for regression transfer,” in *Proceedings of International Conference on Machine Learning*, pp. 863–870, 2010.
- [91] C. Cortes, M. Mohri, and A. M. Medina, “Adaptation based on generalized discrepancy,” *Journal of Machine Learning Research*, vol. 20, no. 1, pp. 1–30, 2019.
- [92] D. Lopez-paz, J. M. Hernández-lobato, and B. Schölkopf, “Semi-supervised domain adaptation with non-parametric copulas,” in *Advances in Neural Information Processing Systems* 25, pp. 665–673, 2012.
- [93] Y. LeCun, Y. Bengio, and G. Hinton, “Deep learning,” *Nature*, vol. 521, no. 7553, pp. 436–444, 2015.
- [94] R. M. Rifkin and R. A. Lippert, “Notes on regularized least squares,” tech. rep., 2007. <http://128.30.100.62:8080/media/fb/ps/MIT-CSAIL-TR-2007-025.pdf>.
- [95] C. Cortes and M. Mohri, “Domain adaptation and sample bias correction theory and algorithm for regression,” *Theoretical Computer Science*, vol. 519, pp. 103–126, 2014.
- [96] H. Liu, M. Long, J. Wang, and Y. Wang, “Learning to adapt to evolving domains,” in *Advances in Neural Information Processing Systems* 33, 2020.
- [97] A. Kumar, T. Ma, and P. Liang, “Understanding self-training for gradual domain adaptation,” in *Proceedings of International Conference on Machine Learning*, pp. 5468–5479, 2020.
- [98] S. Gamrian and Y. Goldberg, “Transfer learning for related reinforcement learning tasks via image-to-image translation,” in *Proceedings of International Conference on Machine Learning*, pp. 2063–2072, 2019.
- [99] P. Gardner, X. Liu, and K. Worden, “On the application of domain adaptation in structural health monitoring,” *Mechanical Systems and Signal Processing*, vol. 138, no. 106550, 2020.